# Omega-3 and -6 fatty acids allocate somatic and germline lipids to ensure fitness during nutrient and oxidative stress in *Caenorhabditis elegans*

Dana A. Lynn[a,b], Hans M. Dalton[a,b], Jessica N. Sowa[c], Meng C. Wang[c], Alexander A. Soukas[d], and Sean P. Curran[a,b,1]

[a]Davis School of Gerontology, University of Southern California, Los Angeles, CA 90089; [b]Dornsife College of Letters, Arts, and Sciences, Department of Molecular and Computational Biology, University of Southern California, Los Angeles, CA 90089; [c]Department of Molecular and Human Genetics, Huffington Center on Aging, Baylor College of Medicine, Houston, TX 77030; and [d]Center for Human Genetic Research and Diabetes Unit, Department of Medicine, Massachusetts General Hospital, Boston, MA 02114

Edited by Gary Ruvkun, Massachusetts General Hospital, Boston, MA, and approved November 9, 2015 (received for review July 16, 2015)

**Animals in nature are continually challenged by periods of feast and famine as resources inevitably fluctuate, and must allocate somatic reserves for reproduction to abate evolutionary pressures. We identify an age-dependent lipid homeostasis pathway in *Caenorhabditis elegans* that regulates the mobilization of lipids from the soma to the germline, which supports fecundity but at the cost of survival in nutrient-poor and oxidative stress environments. This trade-off is responsive to the levels of dietary carbohydrates and organismal oleic acid and is coupled to activation of the cytoprotective transcription factor SKN-1 in both laboratory-derived and natural isolates of *C. elegans*. The homeostatic balance of lipid stores between the somatic and germ cells is mediated by arachidonic acid (omega-6) and eicosapentaenoic acid (omega-3) precursors of eicosanoid signaling molecules. Our results describe a mechanism for resource reallocation within intact animals that influences reproductive fitness at the cost of somatic resilience.**

soma | germline | trade-off | lipids | survival

Trade-offs between fecundity and viability fitness components are thought to drive life-history traits when resources are limited (1). In *Caenorhabditis elegans*, previous studies that removed proliferating germ cells led to an increase in somatic fat (2) and a ∼60% increase in lifespan (3), which is hypothesized to result from the reallocation of germline resources to the soma, promoting survival through enhanced proteostasis (4) and attuned metabolism (5).

Although these previous studies are compelling, the use of reproduction-deficient animals confounds the interpretation of their results with regard to trade-off models, and raises the question of how altered reallocation may affect intact animals. During reproduction, somatic resources are deposited to the germline by the actions of vitellogenins (6), which assemble and transport lipids in the form of yolk from the intestine to developing oocytes. The increased survival of germline-defective animals and their accumulation of somatic lipids suggest that the levels of somatic and germline lipids may influence the age-related decline of somatic cell function in postreproductive life (5). The mechanisms that regulate the distribution of energy resources remain elusive, however.

SKN-1 is the worm homolog of mammalian Nrf2, a cytoprotective transcription factor that impacts multiple aspects of animal physiology (7). Early work on SKN-1 defined its essential roles in development (8) and oxidative stress responses (9), whereas more recent work has identified a role mediating changes in diet availability and composition (10, 11). In the present study, we examined the SKN-1–mediated dietary adaptation pathways (10–12) of *C. elegans* and uncovered a sophisticated mechanism for mobilizing somatic lipids to the germline when animals sense stressful environments. This altruistic act by the soma impacts organismal viability to promote fecundity during oxidative and nutrient stress conditions. The universality of oxidative stress responses among aerobic organisms is a tantalizing source of energetic "cost" to maintain homeostasis that can compete with resources for reproduction. As such, an understanding of how oxidative stress responses impact reproduction, and vice versa, will likely yield insights into how the complex regulation of survival and reproduction trade-offs depend on resource reallocation (13). Here we report a SKN-1–dependent axis of regulating the distribution of somatic and germ cell resources.

## Results

**Age-Dependent Somatic Depletion of Fat Is Induced by Activated SKN-1.** Over the course of an individual's lifespan, lipids are continually mobilized to afford organismal energy demands for growth, cellular maintenance and repair, and reproduction (14). We first examined total fat stores by Oil-red-O (15) (*SI Appendix*, Fig. S1 *A–E*) and fixed Nile red (*SI Appendix*, Fig. S2 *A–D*) in the standard wild type (WT) laboratory *C. elegans* strain N2-Bristol throughout reproduction, from early adulthood (72 h postfeeding) through reproductive senescence (144 h postfeeding). (Herein, hours postfeeding refers to the amount of time that animals have been provided with food following synchronization at larval stage 1 via starvation from hatching.) In these animals, similar to most metazoans, somatic lipid stores increased throughout this time period (Fig. 1 *A* and *B* and *SI Appendix*, Figs. S1 *A–E* and S2 *A–D*).

### Significance

**Food availability in nature changes continually over an organism's lifetime. As such, animals must diligently assess resource availability and appropriately allocate reserves that have been stored during times of feast for reproduction, to abate evolutionary pressures during times of famine. Our findings functionally link the availability of somatic (survival-promoting) and germline (reproduction-promoting) lipids to SKN-1 responses to oxidative and nutrient stress. We have defined this physiological response at the molecular, genetic, and organismal levels and identified a specific signaling system for regulating this process within intact animals. These findings will inform not only laboratory-based studies, but also ecological studies that have long sought to functionally integrate oxidative stress responses (like the SKN-1 pathway) into life-history traits.**

Author contributions: S.P.C. designed research; D.A.L., H.M.D., A.A.S., and S.P.C. performed research; D.A.L., H.M.D., J.N.S., M.C.W., A.A.S., and S.P.C. contributed new reagents/analytic tools; D.A.L., H.M.D., A.A.S., and S.P.C. analyzed data; and S.P.C. wrote the paper.

The authors declare no conflict of interest.

This article is a PNAS Direct Submission.

Freely available online through the PNAS open access option.

[1]To whom correspondence should be addressed. Email: spcurran@usc.edu.

This article contains supporting information online at www.pnas.org/lookup/suppl/doi:10.1073/pnas.1514012112/-/DCSupplemental.

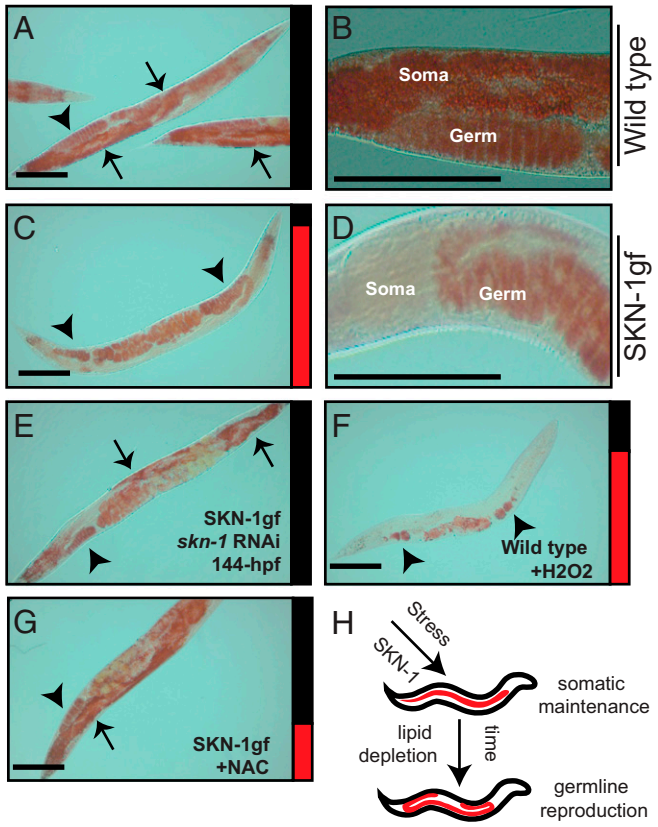


**Fig. 1.** SKN-1 activation mobilizes somatic fat to the germline. (*A–D*) Oil-red-O staining of somatic and germline lipids in WT animals, but only germline lipids in SKN-1gf mutants, at 144 h postfeeding. (*E*) *skn-1* RNAi suppresses Asdf in SKN-1gf animals. (*F*) Asdf is induced in WT animals by acute exposure to $H_2O_2$. (*G*) NAC treatment suppresses Asdf in SKN-1gf animals. (*H*) Cartoon of the Asdf phenotype. Arrows indicate soma, and arrowheads indicate germ. Bar graphs accompanying each panel indicate the percent of population scored with the Asdf phenotype (red) vs. normal lipid distribution (black) from a minimum of two biological replicates for each genotype and condition (*SI Appendix*, Fig. S3). (Scale bars: 100 μm.)

Based on the recent discovery that SKN-1 can potently influence the ability of organisms to metabolically adapt to changes in the environment (10, 11), we next looked at total fat stores during reproduction in SKN-1 gain-of-function (gf) mutant animals (Fig. 1 *C* and *D* and *SI Appendix*, Figs. S1 *A* and *F–M* and S2 *E–L*) and observed the *skn-1*–dependent rapid depletion of somatic, but not germline, lipid stores near the end of the reproductive period (Fig. 1 *C* and *D* and *SI Appendix*, Fig. S1 *I* and *M*, Fig. S2 *H* and *L*, and Table S1), a phenotype that, based on its characteristics, we call the age-dependent somatic depletion of fat (Asdf) phenotype. We assessed the Asdf phenotype in each cohort by quantifying the number of animals that displayed Asdf with those that did not. *SI Appendix*, Fig. S3 provides all % Asdf measurements. The Asdf phenotype was similar in all SKN-1–activating mutants tested, which includes strains harboring mutations in *alh-6* (10, 11) (*SI Appendix*, Fig. S4 *A* and *B*) or *wdr-23* (16) (*SI Appendix*, Fig. S4 *C* and *D*), whereas *skn-1* RNAi suppressed Asdf in SKN-1gf mutant animals (Fig. 1*E*). These data indicate that activated SKN-1 is sufficient to induce Asdf.

SKN-1 activation is correlated with increased levels of reactive oxygen species from endogenous sources or environmental exposure to oxidizing agents (17). Following acute exposure to $H_2O_2$, which can activate SKN-1, WT animals rapidly (within 12 h) deplete most somatic lipids (Fig. 1*F*). The Asdf response is not a generalized stress response and is specific to oxidative stress; WT animals exposed to heat (*SI Appendix*, Fig. S4*G*) or osmotic (*SI Appendix*, Fig. S4*H*) stress environments did not induce the lipid depletion phenotype. Further supporting the need for *skn-1* in the Asdf response, *skn-1*(−/−) null mutants did not deplete somatic fat following $H_2O_2$ exposure, and heterozygous *skn-1*(+/−) animals showed an intermediate response (*SI Appendix*, Fig. S4 *I* and *J*). Asdf was suppressed when animals with activated SKN-1 were treated with the antioxidant *N*-acetylcysteine (NAC) (Fig. 1*G* and *SI Appendix*, Fig. 4 *K–N*). Intriguingly, treatment of WT animals with NAC or *skn-1* RNAi led to excessive accumulation of somatic lipids (*SI Appendix*, Fig. S4 *O–R*), similar to the increased fat observed in *skn-1*(−/−) animals (*SI Appendix*, Fig. S4 *S* and *T*) and consistent with previous reports of lipid phenotypes in animals with reduced *skn-1* (18). This finding supports previous predictions in the life-history theory proposing that the energetic costs to maintain organismal oxidative stress capacity over the animal's lifetime represent a major trade-off variable (19). Taken together, our data indicate that the somatic depletion phenotype is sensitive to oxidative stress and requires SKN-1 (Fig. 1*H*).

**Asdf Mobilizes Somatic Lipids During Nutrient Stress.** Our observation that animals with Asdf retained lipids in the germline suggests that Asdf might result from mobilization of stored somatic lipids to the reproductive system. Members of the vitellogenin family of proteins facilitate transport of stored lipids from the intestine to developing oocytes (20) (Fig. 2*A*). RNAi of all *vit* genes tested resulted in suppression of Asdf (i.e., restoration of somatic lipids), indicating that vitellogenesis is required for Asdf in the SKN-1gf mutants (Fig. 2*B* and *SI Appendix*, Fig. S5 *A–D*). The presence of somatic lipids in SKN-1gf animals was restored

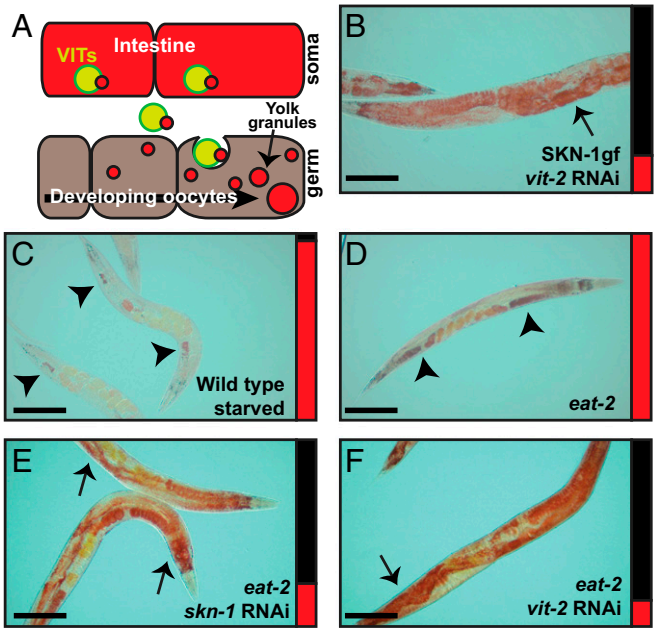


**Fig. 2.** Asdf is a starvation response dependent on vitellogenesis. (*A*) Cartoon representation of the vitellogenin lipid transport system from the intestine to the germline. (*B*) *vit-2* RNAi suppresses Asdf in SKN-1gf animals. (*C*) WT animals starved for 24 h deplete somatic lipids but retain a lipid pool in the germline. (*D*) *eat-2(ad456)* mutants display Asdf at 144 h postfeeding. (*E* and *F*) *skn-1* (*E*) and *vit-2* (*F*) RNAi suppresses Asdf in *eat-2* mutant animals. Arrows indicate soma, and arrowheads indicate germ. Bar graphs accompanying each panel indicate the percent of population scored with the Asdf phenotype (red) vs. normal lipid distribution (black) from a minimum of two biological replicates for each genotype and condition (*SI Appendix*, Fig. S3). (Scale bars: 100 μm.)

CELL BIOLOGY

when *vit-2*, *-3*, or *-5* was targeted by RNAi, or was even increased with reduced expression of *vit-4*. As such, the age-dependent loss of lipids in the soma in SKN-1gf animals is not simply the result of somatic utilization, but rather is a consequence of the unidirectional mobilization of stored lipids by the vitellogenins.

SKN-1 activity is essential for the longevity response to dietary deficiencies (21), and starvation itself can induce oxidative stress (22). Indeed, the depletion of stored lipids in WT animals after 24 h of starvation, albeit more extreme, resembled the Asdf observed in well-fed animals with activated SKN-1 (Fig. 2*C*). Consistent with the idea that the Asdf phenotype in SKN-1gf is a response to a perceived nutritional deficiency, *eat-2* mutants, which eat significantly less food than WT animals (23), also displayed Asdf at the same time point in their reproductive span, whereas WT animals failed to display Asdf (Fig. 2*D* and *SI Appendix*, Fig. S6 *A–D*). Asdf was not observed in *daf-2*/insulin-IGF1 receptor (*SI Appendix*, Fig. S6 *E* and *F*) and *isp-1*/mitochondrial iron sulfur protein (*SI Appendix*, Fig. S6 *G–J*) mutants, and thus is not universal to all longevity-promoting mutations. The Asdf phenotype observed in *eat-2* mutants was suppressed by *skn-1* (Fig. 2*E*) and *vit-2* (Fig. 2*F*) RNAi-treated animals. Note that Asdf is suppressed by the HT115 diet and glucose; thus, all RNAi experiments reported herein were performed in an OP50-background RNAi strain (*SI Appendix*, Fig. S7 and Tables S2 and S3). Our findings support an intriguing model of resource reallocation between the *C. elegans* soma and germline, where activation of the cytoprotective transcription factor SKN-1 under limited food and oxidative stress leads to the mobilization of stored lipid pools to the germline, presumably to ensure fitness.

**Oleic Acid Deficiency Is Sufficient to Induce Asdf.** To understand the mechanisms underlying Asdf, we identified the specific lipid molecules altered in the SKN-1gf mutants by HPLC/GCMS (*SI Appendix*, Fig. S8 *A* and *B*). We noted a significant reduction in C17-branched fatty acids and the monounsaturated fatty acid (MUFA) oleic acid (C18:1 n-9) in the triglyceride fraction of the SKN-1gf mutants compared with WT animals. Oleic acid was the sole lipid species restored to WT levels in SKN-1gf animals when the Asdf phenotype was suppressed by dietary glucose (*SI Appendix*, Figs. S7 *R–U* and S8*C*). *C. elegans* can synthesize oleic acid and all polyunsaturated fatty acid (PUFA) species from dietary or de novo synthesized C16:0 (24) (*SI Appendix*, Figs. S8*D* and S9*A*).

*fat-6* and *fat-7* encode the major isoforms of the Δ9 desaturases that convert stearic acid to oleic acid (25). We subsequently tested for a direct relationship between oleic acid and Asdf. First, we decreased *fat-6*/*-7* by RNAi in WT animals, which phenocopied the Asdf phenotype at the same 144-h postfeeding time point observed in the SKN-1gf mutants (Fig. 3*A*). We measured *fat-6* and *fat-7* mRNA in SKN-1gf and WT animals and found similar levels of expression. Thus, the Asdf phenotype in SKN-1gf mutant animals is not due simply to reduced expression of the transcripts (*SI Appendix*, Table S4). Next, we supplemented the OP50 diet fed to SKN-1gf mutants with 160 μM and 320 μM oleic acid and observed a concentration-dependent reversal of Asdf, with 60.7% and 81.6% suppression of the Asdf phenotype, respectively, in this population (Fig. 3*B* and *SI Appendix*, Fig. S9 *B–G*).

To test the hypothesis that the suppression of Asdf by oleic acid is related to a general increase in total lipids, we assessed the ability of additional lipid supplements to suppress Asdf. We tested lipid species that are biosynthetic precursors to oleic acid, including C18:0 stearic acid (Fig. 3*C* and *SI Appendix*, Fig. S9*H*) and C12:0 lauric acid (*SI Appendix*, Fig. S9 *I* and *J*), as well lipids that are further desaturated products of oleic acid, including C18:2 n-6 linoleic acid, C18:3 n-3 α-linolenic acid, and C18:3 n-6 γ-linolenic acid. Similar to supplementation with stearic and lauric acid, each of these supplements dramatically increased total fat in WT animals; however, they could not suppress Asdf in SKN-1gf mutants (*SI Appendix*, Fig. S9 *K–P*). We also tested

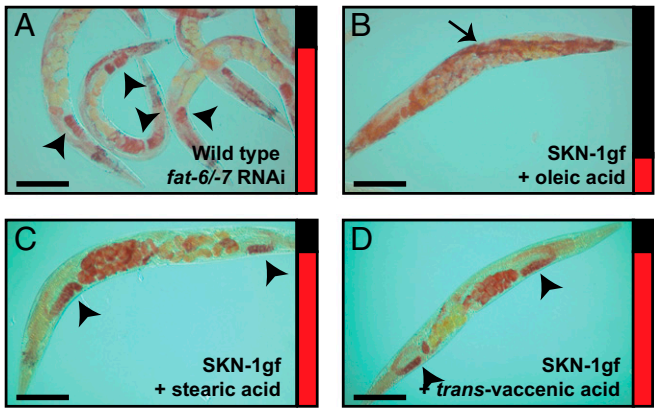


**Fig. 3.** Oleic acid deficiency is causal for Asdf. (*A*) RNAi inactivation of *fat-6*/*-7* in WT animals is sufficient to induce Asdf. (*B*) Dietary supplementation of oleic acid suppresses Asdf in SKN-1gf mutant animals. (*C* and *D*) Dietary supplementation of stearic acid (*C*) and *trans*-vaccenic acid (*D*) do not suppress Asdf in SKN-1gf mutant animals. Arrows indicate soma, and arrowheads indicate germ. Bar graphs accompanying each panel indicate the percent of population scored with the Asdf phenotype (red) vs. normal lipid distribution (black) from a minimum of two biological replicates for each genotype and condition (*SI Appendix*, Fig. S3). (Scale bars: 100 μm.)

*trans*-vaccenic acid (C18:1 *trans*-11), a MUFA that can be desaturated by FAT-6 and FAT-7 (26), but found that, unlike oleic acid, it was incapable of any observable suppression of Asdf in the SKN-1gf mutants (Fig. 3*D* and *SI Appendix*, Fig. S9*Q*). Taken together, these findings suggest that a lipid deficiency, specifically in oleic acid (C18:1), is causal for the Asdf phenotype in SKN-1gf animals as animal reproduction declines.

**Omega-3 and -6 C20 PUFAs Oppose Asdf.** We were surprised to find that lipid defects in the SKN-1gf mutant animals were specific to a single MUFA, oleic acid, and that this defect did not propagate to longer and more unsaturated species (*SI Appendix*, Fig. S8*A*). However, in our assessment of the lipid biosynthesis pathways, we uncovered a role for specific C20 omega-3 and omega-6 PUFAs in the regulation of Asdf. Like mammals, *C. elegans* synthesize a variety of lipid signaling molecules that are epoxy and hydroxyl derivatives of dihomo-γ-linolenic acid (DGLA), arachidonic acid (ARA), and eicosapentaenoic acid (EPA) PUFAs, which influence complex physiological processes that maintain homeostasis (27, 28) (Fig. 4*A*). DGLA and eicosatetraenoic acid (ETA) are biosynthetic precursors for ARA and EPA, respectively; however, ARA can be further desaturated to make EPA, and thus DGLA is a precursor for both ARA and EPA. *fat-4(wa14); fat-1(wa9)* double-mutant animals, which cannot generate ARA or EPA (29), prominently displayed Asdf at the same 144-h postfeeding time point, but not early in reproduction at 72 h postfeeding, as was observed in SKN-1gf mutant animals (Fig. 4*B* and *SI Appendix*, Fig. S10*A*). The levels of *fat-1* and *fat-4* were similar in SKN-1gf and WT animals, indicating that the Asdf phenotype is not due to a reduction in gene expression in SKN-1gf mutant animals (*SI Appendix*, Table S4).

The foregoing data suggest that one function of C20 omega-3 and omega-6 PUFAs is to help maintain the distribution of somatic and germline lipids, and that reduced levels of these lipid species promote Asdf. Treatment of SKN-1gf mutants with 160 μM or 320 μM ARA resulted in potent suppression of Asdf, by 82% and 91%, respectively (Fig. 4*C* and *SI Appendix*, Fig. S10 *B–E*). Similarly, EPA supplementation suppressed Asdf to 40% and 54% of animals at the same concentrations (Fig. 4*D* and *SI Appendix*, Fig. S10 *F* and *G*). The suppression of Asdf was specific to ARA and EPA; SKN-1gf mutants fed OP50 supplemented with DGLA or ETA, even at high concentrations, still

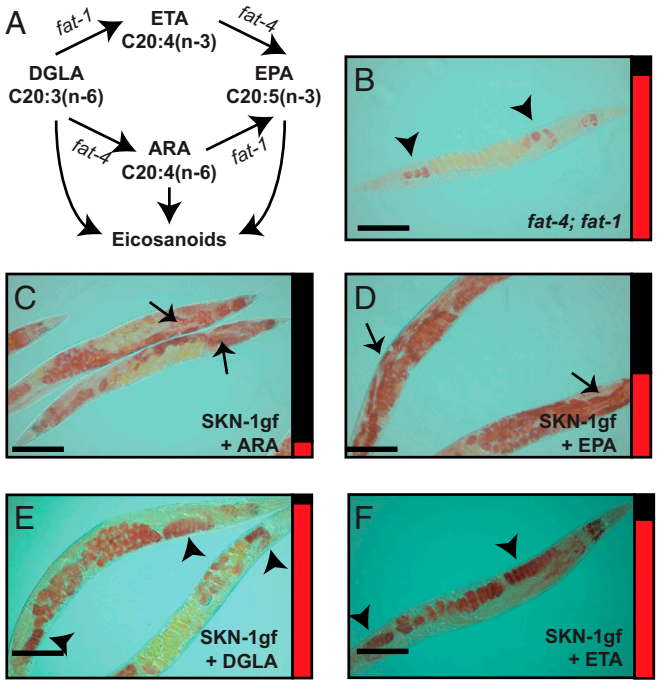


**Fig. 4.** ARA (omega-6) and EPA (omega-3) fatty acids regulate Asdf. (*A*) Schematic of eicosanoid biosynthesis pathways in *C. elegans*. (*B*) ARA and EPA deficient *fat-4(wa14); fat-1(wa9)* animals induce Asdf at 144 h postfeeding. (*C–F*) Dietary supplementation of ARA (*C*) or EPA (*D*), but not of DGLA (*E*) or ETA (*F*), can suppress Asdf in SKN-1gf mutant animals. Arrows indicate soma, and arrowheads indicate germ. Bar graphs accompanying each panel indicate the percent of population scored with the Asdf phenotype (red) vs. normal lipid distribution (black) from a minimum of two biological replicates for each genotype and condition (*SI Appendix*, Fig. S3). (Scale bars: 100 μm.)

displayed Asdf (Fig. 4 *E* and *F* and *SI Appendix*, Fig. S10 *H–J*). Taken together, these findings further support a dose-dependent role for specific omega-6 and omega-3 PUFAs in the homeostatic balance of somatic and germline lipid reserves.

**Asdf Occurs in Natural Isolates of *C. elegans*.** *C. elegans* represent a species of particularly low genetic diversity at the molecular level (30), and recent work to isolate and document the phenotypes of the ever-expanding library of wild *C. elegans* strains has revealed interesting phenotypic variation among them when cultured under laboratory conditions (31). A dearth of ecological data has hindered a better understanding of the relevance of this variation in the natural context, however (32). We analyzed a small collection of wild isolates of *C. elegans* and examined the abundance of somatic and germline lipids and their propensity for Asdf (*SI Appendix*, Fig. S11 *A–H* and Table S5). None of the wild isolates displayed Asdf at early time points in their reproductive span; however, four of the wild isolate strains tested displayed Asdf at the same 144-h postfeeding time point as animals with activated SKN-1, albeit with varying penetrance. NL7000 and ED3040 had the strongest Asdf phenotype, ED3021 displayed an intermediary phenotype, and ED3049 had a weak Asdf response in this population. RW7000, TR403, CB4856, and CB4869 were most similar to N2-Bristol in that they did not display Asdf at any time point.

Strains NL7000 and RW7000 are isolates of the same strain of *Bergerac* that recently diverged in the laboratory setting. Although derived from the same parental isolate, NL7000 displays Asdf at 144 h postfeeding, whereas RW7000 does not. Moreover, and consistent with the idea that Asdf promotes reproductive fitness, NL7000 animals have more progeny and remain reproductive longer than RW7000 animals (*SI Appendix*, Fig. S11*I*). Taken together, our data suggest that the Asdf phenotype is present in some, but not all, wild *C. elegans* strains, and that the propensity for Asdf may be correlated with reproductive success.

**Asdf Promotes Reproduction at the Cost of Survival.** We next assessed the role of Asdf in animal physiology and the resulting impact of deregulating Asdf capacity. During periods of scarce resources, fertile *C. elegans* hermaphrodites exhibit matricide, an altruistic behavior in which fertilized eggs are held in the uterus and hatch internally, and the resulting larvae feed on the hermaphrodite mother as a nutrient source (33). We observed an intriguing matricide phenomenon that correlated with Asdf in SKN-1gf mutants. When day 3 (120 h postfeeding) adult SKN-1gf mutants with early signs of Asdf were starved for 24 h, they became filled with newly hatched larvae, phenotypically defined as bags of worms (Bag) (Fig. 5*A* and *SI Appendix*, Fig. S12 *A–D*). This is in contrast to day 1 adult (72 h postfeeding) SKN-1gf mutant animals and day 1 or 3 adult WT animals, which have only one, if any, internally hatched larvae after 24 h of starvation. During the 48 h separating these two periods in reproduction, WT *C. elegans* accumulate lipids in their somatic tissues (*SI Appendix*, Figs. S1 *B–E* and S2 *A–D*), whereas SKN-1gf mutants mobilize somatic fat to the germline (*SI Appendix*, Figs. S1 *F–M* and S2 *E–L*). The Bag phenotype observed in day 3 adult SKN-1gf mutants with Asdf could be a consequence of the Asdf-mediated increase in germline lipids.

A primary function of somatic cells is to protect the germline, but this comes at the cost of depleting somatic resources. ARA

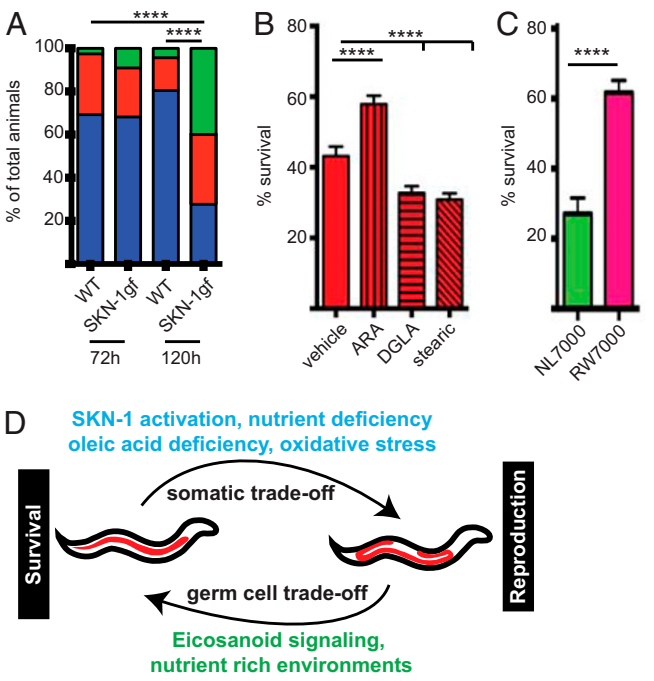


**Fig. 5.** Asdf fuels germ cell maturation to ensure fitness. (*A*) Following 24 h of starvation, SKN-1gf mutants display an age-dependent increase in the incidence of matricide (Bag phenotype) that coincides with Asdf and is not induced in WT animals when starved for 24 h. Blue indicates zero to one internal progeny; red, two to four internal progeny; green, five or more internal progeny. ****$P <$ 0.0001, ANOVA. (*B*) OP50 diet supplemented with ARA, but not with DGLA or stearic acid, can increase somatic resistance to acute $H_2O_2$ exposure in SKN-1gf mutant animals at 144 h postfeeding. ****$P < 0.0001$, ANOVA. (*C*) Somatic resistance to $H_2O_2$ in NL7000 and RW7000 *Bergerac* strains correlates with Asdf competency. Data are mean ± SEM for at least 40 animals, with a minimum of two biological replicates for each genotype and condition. ****$P < 0.0001$, two-tailed *t* test. (*D*) Model for the mechanisms underlying somatic survival and germline reproduction trade-offs of lipid reallocation within intact animals.

supplementation has been linked to the survival of somatic tissues during starvation and can increase the lifespan of ad libitum-fed WT animals (34). SKN-1gf mutants display significant resilience to $H_2O_2$ exposure in early reproductive life compared with WT animals (*SI Appendix*, Fig. S13 *A* and *B*); however, the afforded resistance to exogenous oxidative stress in SKN-1gf mutants declines at 144 h postfeeding (*SI Appendix*, Fig. S13*B*). We hypothesized that the reduction in somatic energy reserves as lipids are mobilized to the germline during Asdf is causal for the diminished oxidative stress resistance capacity. To test this, we inhibited Asdf by ARA supplementation to the OP50 diet, which resulted in a marked increase in resilience to acute $H_2O_2$ exposure in 144 h postfeeding, but not 80 h postfeeding, SKN-1gf animals (Fig. 5*B* and *SI Appendix*, Fig. S13 *B* and *C*). The restoration of somatic resistance to oxidative stress was specific, because supplementation with DGLA and stearic acid did not increase survival at either time point (Fig. 5*B* and *SI Appendix*, Fig. S13*C*). Intriguingly, postreproductive WT animals, which no longer need to devote as many resources to reproduction, exhibited a significantly increased survival response to acute $H_2O_2$ exposure (*SI Appendix*, Fig. S13*A*).

Finally, we examined somatic stress resistance to $H_2O_2$ in the NL7000 ($Asdf^+$) and RW7000 ($Asdf^-$) *Bergerac* strains. Although both strains had enhanced resistance at 72 h postfeeding (*SI Appendix*, Fig. S13*D*), NL7000 displayed a significant loss of resilience at 144 h postfeeding, whereas RW7000 was more apt to survive acute exposure to $H_2O_2$ (Fig. 5*C*). These findings are consistent with an increased capacity for stress resistance that is fueled by additional somatic resources, and regulated by specific omega PUFAs.

Taken together, our results describe a pathway for the reallocation of resources between the soma and germ cells of an intact organism (Fig. 5*D*). Our findings link the availability of somatic and germline lipids to SKN-1 responses to oxidative stress and nutrient limitation. This reallocation impacts somatic survival during stress and reproductive output, which may have universal implications for organisms with specialized soma and germ cells.

## Discussion

In the present study, we examined organismal age-related levels of lipids during the *C. elegans* reproductive span and found a remarkable lipid reallocation phenotype between somatic and germ cells that impacts survival and reproduction trade-offs. We used Oil-red-O and Nile red staining of fixed animals, because the former allows for qualitative assessment of tissue distribution and the latter affords more quantitative measurements, albeit with reduced spatial resolution. We observed similar patterns of lipid distribution with either dye, but each could have unique specificity for different lipid species (35, 36), and differences in the intensity and size of the lipid droplets might reflect a change in the composition of lipid molecules affected.

Our discovery was facilitated by a collection of SKN-1gf mutants that we previously characterized as having reduced lipid levels on fat-inducing diets (10, 11), perhaps owing in part to their starvation-like behaviors, despite being fed ad libitum (12). Although resistant to acute exposure to oxidative stress, none of the constitutively activated SKN-1 mutants have proven to be long-lived. This finding is surprising, given that SKN-1 is a cytoprotective transcription factor essential for mounting an appropriate stress response. The near-complete depletion of somatic lipid reserves from the soma in the animals could explain this lack of longevity in the SKN-1gf mutants. The eventual depletion of somatic lipids was apparent at 144 h postfeeding, but clear differences in lipid abundance between the somatic and germline cells were obvious by 120 h postfeeding. Our data suggest that following the peak of reproduction, somatic resources are mobilized to the germline, but these resources are effectively "wasted" as animals enter reproductive senescence, because postreproductive animals no longer need to devote as many resources to reproduction. Intriguingly, SKN-1gf mutants do indeed have an extended self-reproductive period that does require Asdf, and thus an intriguing model for the function of Asdf is to promote late reproductive output. Although recent reports have shown that mated *C. elegans* hermaphrodites lose fat after mating, future assessment of the impact of Asdf on the fertility of mated animals will be of great interest, considering that maximal reproductive capacity is limited by sperm production in hermaphrodites (37, 38).

Collectively, our data support a genetic role for *skn-1* in the Asdf phenotype. Further refinement of the role SKN-1 plays in the distribution of somatic and germline lipids will be of particular interest. This work expands the known impact of SKN-1 on organismal physiology beyond its role as a mediator of cellular and organismal stress responses (7). One interpretation of this study is that SKN-1 activity is restricted to the soma, which leads to loss of lipids in this compartment; however, the fact that both SKN-1gf and *eat*-2 mutant animals no longer deplete somatic lipids when vitellogenesis is impaired suggests that mobilization of lipids to the germline is at least partially causal for the loss of somatic lipids. In addition, the supplementation of all lipid species resulted in an increase of somatic fat in WT animals and in SKN-1gf mutants early in reproduction, but only oleic acid, ARA, and EPA could suppress Asdf. The fact that most fatty acid supplements did not impact Asdf but also did not increase somatic stress resistance in the SKN-1gf mutants suggests that the depletion of somatic lipids is not simply a result of increased utilization in the soma.

This lipid reallocation has consequences for both somatic and germline tissues. The enhanced resistance to oxidative stress afforded in the SKN-1gf mutant animals is progressively impaired as animals proceed through reproduction, which correlates with the temporal progression of Asdf. Furthermore, if Asdf is suppressed, then the decline in stress resistance is attenuated. Thus, the reallocation of lipids between the soma and the germline is physiologically relevant, because the ultimate location where the lipids reside impacts the function of that compartment. Although body mass index (BMI) has proven to be an imperfect predictor of human metabolic disease risk (39), recent work has suggested that moderate increases in BMI above "normal" can be protective (40). Perhaps the reduction in mortality resulting from increased somatic reserves is the result of enhanced utilization of those stores for adaptation.

We have identified a role for C20 PUFAs in the mobilization of somatic resources to the germline in the SKN-1gf mutant animals. Dietary supplementation with the omega-6 PUFA ARA and the omega-3 PUFA EPA effectively suppressed Asdf, whereas that with the omega-6 PUFA DGLA did not. ARA, EPA, and DGLA are precursors of specific classes of eicosanoid signaling molecules (41), which play multiple and complex roles in animal physiology. Our finding that only ARA and EPA can suppress Asdf suggests that specific species of eicosanoids could be responsible for the physiological responses that we observed. C20 PUFAs also play a critical role in maintaining membrane fluidity (42), and thus the addition of these C20 PUFAs could alter membrane function and signaling capacity; however, the opposing responses to DGLA compared with ARA and EPA suggest that this is not simply a general disorganization of the lipid bilayer (43). Nevertheless, future assessment of the phospholipid composition of membranes, the signaling pathways that influence Asdf, and the functional consequences of perturbing these components on Asdf capacity and resulting phenotypes will be of great interest.

Although we examined reproductive-stage adults, previous studies of germline starvation responses in developing larvae have documented the scavenging of material from the germline to fuel reproduction (44) and even reproductive diapause (45). The increased germline lipid stores in $Asdf^+$ animals could promote two

non-mutually exclusive outcomes: (*i*) provide additional fuel for the rapid maturation of progeny and (*ii*) provide adequate nutrients to escape diapause initiation and/or maintenance. Alternatively, because SKN-1gf mutants Bag only when starved at the end of the reproductive period, this phenotype could represent a time-dependent failure to decrease ovulation in response to nutrient limitation when SKN-1 is constitutively activated. Nevertheless, because progeny's success is subject to the deposition of maternal factors, and their life-history parameters are sensitive to the experiences of the parental and grandparental generations (46–48), future studies to assess the cumulative effects of Asdf capacity on fitness in successive generations are needed.

We analyzed a collection of natural *C. elegans* isolates from diverse climates that revealed that Asdf capacity is variable in the wild (*SI Appendix*, Table S5). The RW7000 *Bergerac* isolate does not display Asdf and has a diminished reproductive period and brood compared with the recently diverged NL7000 strain, which displays Asdf at 144 h postfeeding and has a much larger brood size and a longer self-reproductive period. The number of SNPs between these strains is unknown, and these strains quite possibly could be significantly divergent from each other because they are classical mutator lines, originally used for the active transposons in their genomes. Nonetheless, in light of our finding that single gene mutations are sufficient to induce Asdf, future assessment of the genomic differences between these two strains and all of the wild isolates tested will be of particular interest.

Our results identify a SKN-1 and eicosanoid signaling pathway that balances somatic lipid mobilization to developing germ cells at the cost of survival. Our study provides insight into the trade-offs resulting from the reallocation of lipid stores within intact animals, which are critically important during nutrient and oxidative stress (Fig. 5*D*). The fundamental similarities of the *C. elegans* and mammalian lipid metabolism and eicosanoid biosynthesis and signaling pathways (41) suggests that the resource reallocation pathways and resulting trade-offs may be conserved.

## Methods

*C. elegans* was cultured by standard techniques at 20 °C unless noted otherwise. Statistical analyses were performed with GraphPad Prism 6 software. Data are presented as mean ± SEM. Data were analyzed with the unpaired Student *t* test and two-way ANOVA. All of the methods used in this study are described in detail in *SI Appendix*.

**ACKNOWLEDGMENTS.** We thank L. Thomas and J. Dietrich for technical support and A. Pradhan and J. Lo for a critical reading of the manuscript. We also thank the *Caenorhabditis* Genetics Center, funded by the National Institutes of Health's Office of Research Infrastructure Programs (P40 OD010440), for providing some strains. Support for this work was provided by the National Institutes of Health (Grant T32AG000037, to D.A.L.; R00AG032308, to S.P.C.; and R01 GM109028, to S.P.C.), the American Heart Association (S.P.C.), an Ellison New Scholar Award (S.P.C.), and the American Federation for Aging Research (S.P.C.).

1. Stearns SC (1992) *The Evolution of Life Histories* (Oxford Univ Press, Oxford, UK).
2. O'Rourke EJ, Soukas AA, Carr CE, Ruvkun G (2009) *C. elegans* major fats are stored in vesicles distinct from lysosome-related organelles. *Cell Metab* 10(5):430–435.
3. Hsin H, Kenyon C (1999) Signals from the reproductive system regulate the lifespan of *C. elegans*. *Nature* 399(6734):362–366.
4. Vilchez D, et al. (2012) RPN-6 determines *C. elegans* longevity under proteotoxic stress conditions. *Nature* 489(7415):263–268.
5. Hansen M, Flatt T, Aguilaniu H (2013) Reproduction, fat metabolism, and life span: What is the connection? *Cell Metab* 17(1):10–19.
6. Schneider WJ (1996) Vitellogenin receptors: Oocyte-specific members of the low-density lipoprotein receptor supergene family. *Int Rev Cytol* 166:103–137.
7. Sykiotis GP, Bohmann D (2010) Stress-activated cap'n'collar transcription factors in aging and human disease. *Sci Signal* 3(112):re3.
8. Bowerman B, Eaton BA, Priess JR (1992) *skn-1*, a maternally expressed gene required to specify the fate of ventral blastomeres in the early *C. elegans* embryo. *Cell* 68(6):1061–1075.
9. Sykiotis GP, Bohmann D (2008) Keap1/Nrf2 signaling regulates oxidative stress tolerance and lifespan in *Drosophila*. *Dev Cell* 14(1):76–85.
10. Pang S, Lynn DA, Lo JY, Paek J, Curran SP (2014) SKN-1 and Nrf2 couple proline catabolism with lipid metabolism during nutrient deprivation. *Nat Commun* 5:5048.
11. Pang S, Curran SP (2014) Adaptive capacity to bacterial diet modulates aging in *C. elegans*. *Cell Metab* 19(2):221–231.
12. Paek J, et al. (2012) Mitochondrial SKN-1/Nrf mediates a conserved starvation response. *Cell Metab* 16(4):526–537.
13. Isaksson CS, Sheldon BC, Uller T (2011) The challenges of integrating oxidative stress into life-history biology. *Bioscience* 61:194–202.
14. Efeyan A, Comb WC, Sabatini DM (2015) Nutrient-sensing mechanisms and pathways. *Nature* 517(7534):302–310.
15. Pino EC, Webster CM, Carr CE, Soukas AA (2013) Biochemical and high- throughput microscopic assessment of fat mass in *Caenorhabditis elegans*. *J Vis Exp* 73:50180.
16. Choe KP, Przybysz AJ, Strange K (2009) The WD40 repeat protein WDR-23 functions with the CUL4/DDB1 ubiquitin ligase to regulate nuclear abundance and activity of SKN-1 in *Caenorhabditis elegans*. *Mol Cell Biol* 29(10):2704–2715.
17. An JH, Blackwell TK (2003) SKN-1 links *C. elegans* mesendodermal specification to a conserved oxidative stress response. *Genes Dev* 17(15):1882–1893.
18. Steinbaugh MJ, et al. (2015) Lipid-mediated regulation of SKN-1/Nrf in response to germ cell absence. *eLife* 4:PMC4541496.
19. Selman C, Blount JD, Nussey DH, Speakman JR (2012) Oxidative damage, ageing, and life-history evolution: Where now? *Trends Ecol Evol* 27(10):570–577.
20. Kimble J, Sharrock WJ (1983) Tissue-specific synthesis of yolk proteins in *Caenorhabditis elegans*. *Dev Biol* 96(1):189–196.
21. Bishop NA, Guarente L (2007) Two neurons mediate diet restriction-induced longevity in *C. elegans*. *Nature* 447(7144):545–549.
22. Scherz-Shouval R, et al. (2007) Reactive oxygen species are essential for autophagy and specifically regulate the activity of Atg4. *EMBO J* 26(7):1749–1760.
23. Raizen DM, Lee RY, Avery L (1995) Interacting genes required for pharyngeal excitation by motor neuron MC in *Caenorhabditis elegans*. *Genetics* 141(4):1365–1382.
24. Watts JL (2009) Fat synthesis and adiposity regulation in *Caenorhabditis elegans*. *Trends Endocrinol Metab* 20(2):58–65.
25. Brock TJ, Browse J, Watts JL (2006) Genetic regulation of unsaturated fatty acid composition in *C. elegans*. *PLoS Genet* 2(7):e108.
26. Watts JL, Browse J (2000) A palmitoyl-CoA-specific delta9 fatty acid desaturase from *Caenorhabditis elegans*. *Biochem Biophys Res Commun* 272(1):263–269.
27. Delmastro-Greenwood M, Freeman BA, Wendell SG (2014) Redox-dependent anti-inflammatory signaling actions of unsaturated fatty acids. *Annu Rev Physiol* 76:79–105.
28. Kosel M, et al. (2011) Eicosanoid formation by a cytochrome P450 isoform expressed in the pharynx of *Caenorhabditis elegans*. *Biochem J* 435(3):689–700.
29. Vásquez V, Krieg M, Lockhead D, Goodman MB (2014) Phospholipids that contain polyunsaturated fatty acids enhance neuronal cell mechanics and touch sensation. *Cell Reports* 6(1):70–80.
30. Sivasundar A, Hey J (2003) Population genetics of *Caenorhabditis elegans*: The paradox of low polymorphism in a widespread species. *Genetics* 163(1):147–157.
31. de Bono M, Bargmann CI (1998) Natural variation in a neuropeptide Y receptor homolog modifies social behavior and food response in *C. elegans*. *Cell* 94(5):679–689.
32. Barrière A, Félix MA (2014) Isolation of *C. elegans* and related nematodes. *WormBook*, doi/10.1895/wormbook.1.115.2.
33. McCulloch D, Gems D (2003) Evolution of male longevity bias in nematodes. *Aging Cell* 2(3):165–173.
34. O'Rourke EJ, Kuballa P, Xavier R, Ruvkun G (2013) Omega-6 polyunsaturated fatty acids extend life span through the activation of autophagy. *Genes Dev* 27(4):429–440.
35. Greenspan P, Mayer EP, Fowler SD (1985) Nile red: A selective fluorescent stain for intracellular lipid droplets. *J Cell Biol* 100(3):965–973.
36. Rudolf M, Curcio CA (2009) Esterified cholesterol is highly localized to Bruch's membrane, as revealed by lipid histochemistry in whole mounts of human choroid. *J Histochem Cytochem* 57(8):731–739.
37. Shi C, Murphy CT (2014) Mating induces shrinking and death in *Caenorhabditis* mothers. *Science* 343(6170):536–540.
38. Hodgkin J, Barnes TM (1991) More is not better: Brood size and population growth in a self-fertilizing nematode. *Proc Biol Sci* 246(1315):19–24.
39. Conus F, Rabasa-Lhoret R, Peronnet F (2007) Characteristics of metabolically obese normal-weight (MONW) subjects. Appl Physiol Nutr Metab 32(1):4–12.
40. Flegal KM, Kit BK, Orpana H, Graubard BI (2013) Association of all-cause mortality with overweight and obesity using standard body mass index categories: A systematic review and meta-analysis. *JAMA* 309(1):71–82.
41. Vrablik TL, Watts JL (2013) Polyunsaturated fatty acid derived signaling in reproduction and development: Insights from *Caenorhabditis elegans* and *Drosophila melanogaster*. *Mol Reprod Dev* 80(4):244–259.
42. Watts JL, Browse J (2002) Genetic dissection of polyunsaturated fatty acid synthesis in *Caenorhabditis elegans*. *Proc Natl Acad Sci USA* 99(9):5854–5859.
43. Webster CM, Deline ML, Watts JL (2013) Stress response pathways protect germ cells from omega-6 polyunsaturated fatty acid-mediated toxicity in *Caenorhabditis elegans*. *Dev Biol* 373(1):14–25.
44. Seidel HS, Kimble J (2011) The oogenic germline starvation response in *C. elegans*. *PLoS One* 6(12):e28074.
45. Angelo G, Van Gilst MR (2009) Starvation protects germline stem cells and extends reproductive longevity in *C. elegans*. *Science* 326(5955):954–958.
46. Greer EL, Brunet A (2009) Different dietary restriction regimens extend lifespan by both independent and overlapping genetic pathways in *C. elegans*. *Aging Cell* 8(2):113–127.
47. Rechavi O, et al. (2014) Starvation-induced transgenerational inheritance of small RNAs in *C. elegans*. *Cell* 158(2):277–287.
48. Pang S, Curran SP (2012) Longevity and the long arm of epigenetics: Acquired parental marks influence lifespan across several generations. *BioEssays* 34(8):652–65.

# Supplemental Materials

## Supplemental Text

*C. elegans,* like all organisms, must effectively manage energy reserves throughout their life in order to optimize survival and reproduction[1]. The regulation of fat homeostasis integrates genetic pathways that function in nutrient uptake, storage, and utilization, which have obvious influences on metabolism but can also impact reproduction and lifespan[2-8]. The sensing of available nutrients and the metabolic state of the organism can potently influence these physiological pathways. Previous studies have focused on the developmental programs that underlie fat storage capacity[9]; leaving a gap in our understanding of how lipid homeostasis is maintained in later adult stages. In particular, the regulatory mechanisms that balance resources between somatic (survival-promoting) and germ (reproduction-promoting) cells and the resulting physiological consequence of aberrant reallocation within intact animals (functional soma and germline) are largely unknown.

### Asdf is a diet-dependent phenotype

Many metabolic phenotypes are not only sensitive to the amount of food ingested but also integrate information regarding the composition of the diet[5,10-12]. Similar to wild type animals feeding of an HT115/ *E. coli* K-12 bacterial diet increased early reproductive output of the SKN-1gf mutant animals (Fig. S7a and Table S2), but also abolished the extended self-reproduction (Fig. S7b-n and Table S2) period of the SKN-1gf mutants and suppressed the Asdf phenotype (Fig. S7b-n). As such, we adopted an OP50/*E.coli* B strain capable of generating dsRNA for all of our feeding RNAi experiments (Table S3).

We developed a strategy to assess the temporal requirement of the OP50 diet to induce Asdf at 144-hours post feeding (Fig. S7o). The suppression of Asdf was fully penetrant when animals were switched from the OP50 to HT115 diet just prior to adulthood (48-hours post feeding) (Fig. S7p), but the influence of diet was less pronounced - i.e. a small percentage of animals still display Asdf - when the switch to the HT115 diet was done in reproductively active animals (96-hours post feeding) (Fig. S7q), consistent with the prediction that Asdf is important later in reproduction. One major difference in the macronutrient complexity of the HT115 diet is the

high carbohydrate composition as compared to OP50[13]. Intriguingly, supplementation of the OP50 diet with 2% glucose was also capable of suppressing Asdf in the SKN-1gf mutants (Fig. S7r-u), indicating the soma-to-germline mobilization of lipids is sensitive to the abundance of dietary carbohydrates.

The importance of characterizing the specific composition of the diet utilized in physiological measurements is becoming increasingly appreciated[5,10-12]; especially in the context of SKN-1 dependent phenotypes. The proper identification of *skn-1* and the vitellogenin family of genes in the regulation of Asdf required the development of an OP50 (*E. coli* B*)* derived RNAi competent strain, as the high carbohydrate composition of the HT115 diet could potently suppress Asdf. In addition to glucose, we identified an important role for oleic acid in the propensity for animals to display Asdf. Oleic acid levels are directly tied to the availability of carbohydrates in the diet [14]. Importantly, suppression of Asdf by fatty acid supplementation is specific to oleic acid and is not simply a result of making animals fatter. These findings further emphasize the importance of considering the impact that diet will have on the experimental output of all studies and will be of importance to laboratory-based studies and ecological studies examining wild animals and their dietary history.

## Materials and Methods:

### *C. elegans* and *E. coli* strains and culture conditions

*C. elegans* were cultured using standard techniques at 20°C [15] unless otherwise noted. The following strains were used: wild-type N2 Bristol, SPC207: *skn-1(lax120)*, SPC227: *skn-1(lax188)*, SPC321: *alh-6(lax105)*, SPC303: *wdr-23 (lax211)*, VC1772 (*skn-1(ok2315) IV/nT1[qIs51](IV;V)),* BX52: *fat-4(wa14);fat-1(wa9)*, DA453: *eat-2(ad456)*, MQ887: *isp-1(qm150)*, DR1572: *daf-2(e1368)*; natural isolates: NL7000, ED3040, ED3021, TR403, CB4856, CB4869, RW7000, ED3049. Staged animals were obtained by washing animals each day to new plates during the reproductive period, allowing adults to settle by gravity, dropping samples on plates, and burning off any progeny missed in the wash steps.

*E.coli* strains were grown in LB supplemented with appropriate antibiotic(s) for selection. The following strains were used: OP50 – *E.coli* B, ura, OP50-RNAi (described below) *E.coli* B, rnc14::ΔTn10, laczγA::T7pol, HT115(DE3) - Derived from *E. coli* K12, F-, mcrA, mcrB, IN(rrnD-rrnE)1, rnc14::Tn10 (DE3 lysogen: lacUV5 promoter –T7 polymerase). All experiments used plates with freshly seeded *E.coli,* from cultures grown for 16-18 hours (h) "overnight" (O/N) at 37°C, and inoculated from stock plates less than 1-month of age.

### GC-MS

Samples were grown in triplicate on OP50 with and without 2% glucose supplementation (see below). At larval-stage 4 (L4), 7500 animals were washed three times with 1X PBS, then pelleted at 20,000 x *g* and supernatant was aspirated off. Afterwards, samples were promptly frozen at -80°C. Lipid extracts from these samples were analyzed by solid-phase chromatography followed by GCMS as previously reported [5,16]. For all measurements, at least two biological replicates were performed, with data shown as mean ± SEM.

### Lipid staining

Oil-red-O (ORO) or fixed Nile red staining [4] was conducted by washing 200-300 animals from experimental plates synchronized by egg-prep with 1x PBS + 0.01% Triton X-100 (PBST). Worms were washed three times with 1x PBST and allowed to settle by gravity. To permeabilize the cuticle, worms were resuspended in 100µl 1x PBST and 600µl of 40% isopropanol was added while samples were rocked for three minutes. Worms were spun down at 500 RPM for 30s and 600µl was aspirated off. Then, 600µl of 60% ORO working stock solution is added and samples are rotated at room temperature (RT) – 21.0-23.5°C for two hours. ORO working stock was prepared as follows: a 0.5g of ORO in 100mL isopropanol is stirred O/N and on the day of staining, is freshly diluted to 60% with water and rocked for two hours, and debris removed through a 0.22µm-filter. Worm samples are pelleted at 500 RPM for 30s, 600µl of solution is aspirated off, and 600µl of PBST is added. Samples are rotated for another 30 minutes at RT and then animals were mounted on slides in the presence of DAPI (internal control for permeabilization of animals) and imaged with a color camera (Zeiss AxioCam ERc5s) outfitted with DIC optics. A minimum of twenty animals were imaged in a minimum of two independent biological replicates and results were consistent between biological replicates.

### Assessment of Asdf capacity

ORO stained samples were processed as indicated above and images collected. Percent (%) Asdf is quantified by counting the number of animals in a cohort that display the phenotype compared to the number of animals that do not. A minimum of two independent experiments

with 2-3 biological replicates, n=4 to 6 are performed. Although hundreds of animals are examined and scored over all replicates, the calculated % Asdf presented in each figure and Supplemental Fig. 3 only accounts for whole and non-overlapping animals in the field of view and where the germline and soma are clearly defined. Blind scoring of % Asdf in each sample is then independently assessed by two individuals and their results compiled to reflect %Asdf of the population.

**Reproduction assays**

L1 stage animals were synchronized by egg prep, rocked O/N at 20°C, and dropped onto experimental plates the next morning. 48-hours post-feeding, ten L4 stage animals of each strain and diet were moved to their own respective experimental plate. These animals were then assigned a number and their reproductive output was tracked, twice daily, by moving each animal to a fresh plate every twelve hours until reproduction ceased. To ensure accurate counts of progeny number, each plate was assessed at least twice; 24 to 48-h after the hermaphrodite mother was moved from the plate.

**RNAi OP50 strain construction**

RNAi OP50 was created by replacing the WT OP50 allele of RNAIII RNase (rnc) with a deletion allele and introducing an IPTG-inducible T7 RNA polymerase. P1 phage lysates were prepared from strains HT115 (rnc14::ΔTn10) and CH1681(laczγA::T7pol camFRT). To generate the OP50 (rnc14::ΔTn10) strain, an overnight culture of OP50 was transduced with an equal volume of HT115 P1 lysate and plated on LB+tet+citrate plates. Positive colonies were re-selected three times on LB+tet+citrate media plates. Individual colonies were subsequently inoculated into LB+tet and the presence of rnc14::ΔTn10 allele was confirmed by PCR. To generate the RNAi-competent OP50 strain an overnight culture of OP50 (rnc14::ΔTn10) was transduced with equal volume of Ch1681 P1 lysate and selected on LB+cam+citrate plates. Positive colonies were restreaked three times onto LB+cam+citrate media plates. Individual colonies, were subsequently inoculated into LB+tet+cam and the presence of rnc14::ΔTn10 and laczγA::T7pol was confirmed by PCR.

**RNA interference (RNAi)**

An RNAse III-deficient OP50 *E. coli* B strain was engineered for IPTG-inducible expression of T7 polymerase (See above). Sequence verified double stranded RNA-expression plasmids were transformed into this strain. RNAi feeding plates were prepared using standard NGM recipe with 5mM isopropyl-β-D-thiogalactoside (IPTG) and 50 ug/ml carbenicillin. Synchronized L1 animals were added to plates to knockdown indicated genes.

**Lipid feeding (supplementation assays)**

Fatty acid supplementation plates were made using an adapted protocol [17]. In brief, 100mM aqueous solution stocks of each supplement were first made. These were made fresh right before pouring regular NGM plates containing 0.1% tergitol (NP40) and added to NGM media once cooled to 55°C at the concentrations indicated. Oleic acid (#90260), Stearic acid (#10011298), Lauric acid (#10006626), Linoleic acid (#90150), a-linolenic acid (#90210), g-linolenic acid (#90220), *trans*-vaccenic acid (#15301), and DGLA (#90230) were purchased from Cayman Chemical and AA (#A9673) and EPA (#E2011) were purchased from Sigma Aldrich.

**Glucose supplementation**

Glucose was added to NGM media, cooled to 55°C, to obtain a final concentration of 2% glucose in the worm plates.

**Starvation and matricide assays**
Staged adult animals were washed 5 times in 1x PBS to get rid of any food, transferred to 15mL conical tubes, and 10mL of liquid NGM (prepared just like NGM media but without agar) was added to ~50ul of washed worms. Volumes of liquid NGM were adjusted accordingly to make maintain worm density across experiments. Tubes were gently rotated overnight at 20°C and 24 hours later, total lipid (ORO) and the frequency of the Bag phenotype (more than one internally hatched progeny) was assessed by microscopy.

**Oxidative stress assays**
Staged animals were collected and washed with 1x Phosphate Buffered Saline + Triton X-100 (PBST) three times to remove any contamination from the bacterial food source. After the final wash, the animals were allowed to settle, by gravity, and the supernatant was aspirated leaving ~100ul behind. 1mL of H2O2 solution (concentrations ranging between 2mM to 10mM) in 1x PBST was added to each experimental tube of worms. Tubes were gently rotated at RT for 20 minutes, followed by centrifugation at 500 RPM for 30s and the worms were washed three times in 1X PBST. After the final wash animals were dropped onto seeded NGM plates for recovery. Recovery times (as indicated) varied between 12 and 24 hours before analysis. ORO staining and imaging was used for fat depletion analysis while survival was recorded based on head response from prodding with a platinum wire.

**NAC assays**
N-acetyl-cysteine (NAC) solution in water was added to the top of a seeded worm plate at a final concentration of 10mM and allowed to dry in a sterile hood. The solution was made to cover the entirety of the 300ul bacterial lawn. Synchronized animals were moved to these plates at the L1 stage, kept on this diet their whole lives, and then total lipids stained and imaged at the specified times.

**Heat shock assay**
Synchronized L1 wild type animals were raised on normal OP50 bacteria seeded worm plates for 72 hours at 20°C. Then, plates were transferred to 30°C for 9 hours. After that time, plates were transferred back to 20°C and worms were allowed to recover O/N. At 96-hours post feeding, total lipids were stained and imaged. Adapted from Walker et al.[18].

**Osmotic stress assay**
NGM plates were prepared with 11.67g/L of NaCl (instead of 3.0g/L, as normal) for 200mM final concentration and were subsequently seeded with OP50 bacteria. Synchronized wild type animals were moved to these plates at the L1 stage, kept on these plates their whole lives, and then total lipids stained and imaged at 144-hours post feeding. Adapted from Lamitina et al.[19].

**Statistics**
Statistical analyses were performed with GraphPad Prism 6 software. Data are presented as mean±s.e.m. Data were analyzed by using unpaired Student's t-test and two-way ANOVA. $P<0.05$ was considered as significant.

**References**


1 Ashrafi, K. Obesity and the regulation of fat metabolism. *WormBook*, 1-20, doi:10.1895/wormbook.1.130.1 (2007).

2 Curran, S. & Ruvkun, G. Lifespan regulation by evolutionarily conserved genes essential for viability. *PLoS Genet* **3**, e56, doi:10.1371/journal.pgen.0030056 (2007).

3 Tacutu, R. *et al.* Prediction of C. elegans Longevity Genes by Human and Worm Longevity Networks. *PLoS One* **7**, e48282, doi:10.1371/journal.pone.0048282 (2012).

4 O'Rourke, E. J., Soukas, A. A., Carr, C. E. & Ruvkun, G. C. elegans major fats are stored in vesicles distinct from lysosome-related organelles. *Cell Metab* **10**, 430-435, doi:10.1016/j.cmet.2009.10.002 (2009).

5 Soukas, A. A., Kane, E. A., Carr, C. E., Melo, J. A. & Ruvkun, G. Rictor/TORC2 regulates fat metabolism, feeding, growth, and life span in Caenorhabditis elegans. *Genes & development* **23**, 496-511, doi:10.1101/gad.1775409 (2009).

6 Hansen, M., Flatt, T. & Aguilaniu, H. Reproduction, fat metabolism, and life span: what is the connection? *Cell Metab* **17**, 10-19, doi:10.1016/j.cmet.2012.12.003 (2013).

7 Khanna, A., Johnson, D. L. & Curran, S. P. Physiological roles for mafr-1 in reproduction and lipid homeostasis. *Cell reports* **9**, 2180-2191, doi:10.1016/j.celrep.2014.11.035 (2014).

8 Vrablik, T. L. & Watts, J. L. Polyunsaturated fatty acid derived signaling in reproduction and development: insights from Caenorhabditis elegans and Drosophila melanogaster. *Molecular reproduction and development* **80**, 244-259, doi:10.1002/mrd.22167 (2013).

9 Mak, H. Y. Lipid droplets as fat storage organelles in Caenorhabditis elegans: Thematic Review Series: Lipid Droplet Synthesis and Metabolism: from Yeast to Man. *J Lipid Res* **53**, 28-33, doi:10.1194/jlr.R021006 (2012).

10 Maier, W., Adilov, B., Regenass, M. & Alcedo, J. A neuromedin U receptor acts with the sensory system to modulate food type-dependent effects on C. elegans lifespan. *PLoS Biol* **8**, e1000376, doi:10.1371/journal.pbio.1000376 [doi] (2010).

11 Pang, S. & Curran, S. P. Adaptive Capacity to Bacterial Diet Modulates Aging in C. elegans. *Cell Metab* **19**, 221-231, doi:10.1016/j.cmet.2013.12.005 (2014).

12 Pang, S., Lynn, D. A., Lo, J. Y., Paek, J. & Curran, S. P. SKN-1 and Nrf2 couples proline catabolism with lipid metabolism during nutrient deprivation. *Nature communications* **5**, 5048, doi:10.1038/ncomms6048 (2014).

13 Brooks, K. K., Liang, B. & Watts, J. L. The influence of bacterial diet on fat storage in C. elegans. *PLoS One* **4**, e7545, doi:10.1371/journal.pone.0007545 (2009).

14 Merkel, M., Velez-Carrasco, W., Hudgins, L. C. & Breslow, J. L. Compared with saturated fatty acids, dietary monounsaturated fatty acids and carbohydrates increase atherosclerosis and VLDL cholesterol levels in LDL receptor-deficient, but not apolipoprotein E-deficient, mice. *Proc Natl Acad Sci U S A* **98**, 13294-13299, doi:10.1073/pnas.231490498 (2001).

15 Brenner, S. The genetics of Caenorhabditis elegans. *Genetics* **77**, 71-94 (1974).

16 Perez, C. L. & Van Gilst, M. R. A 13C isotope labeling strategy reveals the influence of insulin signaling on lipogenesis in C. elegans. *Cell Metab* **8**, 266-274, doi:10.1016/j.cmet.2008.08.007 (2008).

17 Deline, M. L., Vrablik, T. L. & Watts, J. L. Dietary supplementation of polyunsaturated fatty acids in Caenorhabditis elegans. *J Vis Exp*, doi:10.3791/50879 (2013).

18 Walker, G. A. *et al.* Heat shock protein accumulation is upregulated in a long-lived mutant of Caenorhabditis elegans. *J Gerontol A Biol Sci Med Sci* **56**, B281-287 (2001).
19 Lamitina, T., Huang, C. G. & Strange, K. Genome-wide RNAi screening identifies protein damage as a regulator of osmoprotective gene expression. *Proc Natl Acad Sci U S A* **103**, 12173-12178, doi:10.1073/pnas.0602987103 (2006).

## Supplemental Figure Legends

**Figure S1. ORO Asdf progression in wild type and SKN-1(gf) mutants.**
**(**a) Daily progeny production of OP50-fed wild type (blue circle) and SKN-1gf mutant (red square) animals, $*P < 0.05$, $**P < 0.01$, two-tailed *t* test. Oil-red-O staining of total lipids in (b-e) Wild type, (f-i) SKN-1gf*(lax188)*, and (j-m) SKN-1gf*(lax120)* adult animals during reproduction.

**Figure S2. NR Asdf progression in wild type and SKN-1(gf) mutants.**
Nile red staining of total lipids in (a-d) Wild type, (e-h) SKN-1gf*(lax188)*, and (i-l) SKN-1gf*(lax120)* adult animals during reproduction. Where labeled, arrows point to somatic lipids and arrowheads denote germline lipids in oocytes

**Figure S3. Cohort analysis of %Asdf.**
% Asdf is quantified by counting the number of animals in a cohort that display the phenotype compared to the number of animals that do not. Mean ± SEM, *n* = # of animals used from at two of the biological replicates performed to calculate % Asdf.

**Figure S4. SKN-1 activation and oxidative stress induce Asdf.**
(a-f) SKN-1 activation is sufficient to induce Asdf as observed in (a-b) *alh-6(lax105),* (c-d) *wdr-23(lax211)*, and (e-f) acute exposure to hydrogen peroxide (H2O2), but not (g) heat shock or (h) osmotic stress but is dependent on (i-j) *skn-1*. (k-p) Dietary supplementation of the antioxidant N-acetylcysteine (NAC) suppresses Asdf in (k-l) *alh-6(lax105)* and (m-n) *skn-1(lax188)gf* and increases somatic fat in (o-p) wild type. (q-r) *skn-1* RNAi and (s-t) *skn*-1 null mutants display increased somatic fat as compared to controls.

**Figure S5. Vitellogenin proteins transport lipids from the soma to the germline in animals with Asdf.**
(a-d) Fixed Nile red staining of total lipids in animals treated with RNAi of the vitellogenin family of proteins: (a) control RNAi, (b) *vit-3* RNAi, (c) *vit-4* RNAi, (d) *vit-5* RNAi; suppresses the somatic transfer of lipids to the germline in SKN-1gf animals with Asdf.

**Figure S6. Asdf is a specific response to nutrient deprivation.**
(a-f) Fixed Nile red staining of mutant animals. (a-b) WT, (c-d) *eat-2* mutants in early reproduction do not display Asdf while *eat-2* mutants late in reproduction do display Asdf (d). Long-lived (e-f) *daf-2*(insulin receptor) do not display Asdf. (g-j) Oil red O staining reveals lack of Asdf in (g-h) wild type and (i-j) *isp-1*(mitochondrial iron sulfur cluster protein) mutants. Notes: exposure time for *daf-2* mutants with fixed Nile red fluorescence was 50% of WT as to properly resolve structures. *daf-2* mutant animals were grown at 20C until L2/L3 stage and then moved to 25C, as such 144-h *daf-2* animals are likely developmentally more mature than age-matched controls.

**Figure S7. Asdf is a diet-dependent phenotype.**
(a) An HT115-diet (green square) increases early daily progeny production and suppresses extended self-reproduction observed in SKN-1gf fed an OP50-diet (red square), $**P < 0.01$, $****P < 0.0001$, two-tailed *t* test. (b) The HT115 bacterial diet suppresses Asdf in SKN-1gf

mutant animals at 144-hours post feeding. Oil-red-O staining of total lipids reveals that Asdf does not occur at any time in reproductive life when an HT115-diet is fed to: Wild type (c-f), SKN-1gf*(lax188)* (g-j), or (k-n) SKN-1gf*(lax120)* adult animals. (o) cartoon representation of diet switching experiments. -, not observed; +, 25-50% of population display Asdf, ++, 50-75% of population display Asdf; +++, 75-100% of population display Asdf. (p) Asdf is fully suppressed in OP50-fed SKN-1gf mutants if switched to an HT115 diet at 48-hours post feeding and (q) partially suppressed when switched at 96-hours post feeding. (r) Glucose supplementation of the OP50 bacterial diet suppresses Asdf in SKN-1gf animals. (s-t) 2% Glucose supplementation of the OP50-diet increases somatic lipid stores in WT animals. (u) *skn-1(lax188)gf* mutants accumulate less somatic lipids on a 2% carbohydrate supplemented OP50-diet early in reproduction. Bar graphs accompanying each panel indicate the percent of population scored with the Asdf phenotype (red) versus normal lipid distribution (black) from a minimum of two biological replicates for each genotype and condition (see Fig. S3 for more detail). Scale bars = 100um.

**Figure S8. Oleic acid deficiency in SKN-1gf mutants is reversed by dietary glucose.**
(a) GCMS analysis of total fatty acids in the triglyceride fraction of wild type (blue) and SKN-1gf (red) animals fed an OP50-diet, ****$P < 0.0001$, two-tailed *t* test. (b) GCMS analysis of total fatty acids in the triglyceride fraction of wild type (blue) and *skn-1(lax120)gf* (orange) animals fed an OP50-diet. (c) GCMS analysis of total fatty acids in the triglyceride fraction of: WT fed OP50 (dark blue); WT fed OP50+glucose (light blue), *skn-1(lax188)gf* fed OP50 (red), *skn-1(lax188)gf* fed OP50+glucose (purple), *skn-1(lax120)gf* fed OP50 (orange) and *skn-1(lax120)gf* fed OP50+glucose (yellow) animals. (d) Schematic of oleic acid biosynthetic pathway in *C. elegans*. Abbreviations: cyclo, cyclopropane fatty acid; iso, iso-methyl branched chain fatty acid.

**Figure S9. Oleic acid deficiency is sufficient to induce Asdf.**
(a) Schematic of lipid biosynthesis pathway in *C. elegans.* (b-g) Oleic acid supplementation increases somatic lipids in wild-type and suppresses Asdf in SKN-1gf mutants in a dose dependent manner. Supplementation of stearic acid, lauric acid, linoleic aicd, α-linolenic acid, γ-linolenic acid, or trans-vaccenic acid increases somatic lipids in wild-type (h,i,k,m,o,q) and but does not suppress Asdf in SKN-1gf mutants (j,l,n,p) ****, $P<0.0001$

**Figure S10. AA and EPA precursors of eicosanoid signaling molecules influence Asdf.**
(a) Eicosanoid-deficient *fat-4(wa14); fat-1(wa9)* mutant animals do not display Asdf early in reproduction (72-hpf). (b-e) Arachadonic acid (ARA) supplementation increases somatic lipids in WT and suppressed Asdf in SKN-1gf mutants. (f-g) Eicosapentaenoic acid (EPA) supplementation increases somatic lipids in WT and suppressed Asdf in SKN-1gf mutants. (h) dihomo-γ-linolenic acid (DGLA) and (i) Eicosatetraenoic acid (ETA) increases somatic lipids in WT as compared to controls (j).

**Figure S11. Variation of Asdf among natural isolates of *C. elegans*.** Oil-red-O staining of somatic and germline lipids reveals Asdf-capacity (a-d) and -deficiency (e-h) among isolated natural isolates of *C. elegans* at 144-hours post feeding. (i) Daily progeny output of NL7000 (blue circles) and RW7000 (red squares) isolates of *C. elegans Bergerac* strains, *$P < 0.05$, **$P < 0.01$, two-tailed *t* test.. Bar graphs accompanying each panel indicate the percent of

population scored with the Asdf phenotype (red) versus normal lipid distribution (black) from a minimum of two biological replicates for each genotype and condition (see Fig. S3 for more detail). Scale bars = 100um.

**Figure S12. Matricide is enhanced in animals with Asdf after 24-hours of starvation.**
WT animals in early (a) and late (b) reproductive life do not Bag (> 1 internally hatched worm) after 24-hours of starvation. (c) SKN-1gf mutants, early in reproductive life do not Bag when starved for 24-hours. (d) SKN-1gf mutants, with Asdf, late in reproductive life display a high incidence of matricide when starved for 24-hours. Arrows denote internally hatched larvae.

**Figure S13. Survival of acute exposure to hydrogen peroxide is influenced by Asdf.**
(a) WT animals early in reproduction are sensitive to acute exposure to H2O2 and more resistant at the end of the reproductive period. (b) SKN-1gf mutant animals are resistant to acute exposure to H2O2 and that resistance declines later in reproduction, which correlates with Asdf. (c) Supplementation of stearic acid or DGLA does not increase somatic resistance to H2O2 early or late in reproduction in SKN-1gf mutants. (d) NL7000 and RW7000 *Bergerac* strains are resistant to H2O2 oxidative stress early in reproduction. ****, $P<0.0001$ two-tailed *t* test.

**Table S1**. **Daily progeny production for wild type and SKN-1gf on the OP50 diet**

| | **Hours post feeding (hpf)** | | | | | | | | | | |
|---|---|---|---|---|---|---|---|---|---|---|---|
| | **60** | **72** | **84** | **96** | **108** | **120** | **132** | **144** | **156** | **168** | **TOTAL** |
| WT-1 | 8 | 25 | 50 | 48 | 31 | Censor[1] | | | | | 162 |
| WT-2 | 28 | 21 | 38 | 37 | 45 | Censor[1] | | | | | 169 |
| WT-3 | 10 | 26 | 36 | 67 | 58 | 13 | 0 | 1 | 0 | 1 | 212 |
| WT-4 | 0 | 26 | 42 | 39 | 72 | 49 | 39 | 6 | 0 | 0 | 273 |
| WT-5 | 11 | 43 | 68 | 66 | 77 | 8 | 2 | 0 | 1 | 0 | 276 |
| WT-6 | 9 | 17 | 37 | 46 | 53 | 29 | 0 | 0 | 2 | 1 | 194 |
| WT-7 | 18 | 41 | 48 | 37 | 65 | 35 | 14 | 15 | 9 | 7 | 289 |
| WT-8 | 3 | 51 | 69 | 81 | 59 | 5 | 1 | 0 | 0 | 0 | 269 |
| WT-9 | 0 | 22 | 56 | 64 | 75 | 70 | 4 | 2 | 0 | 0 | 293 |
| WT-10 | 0 | 31 | 63 | 90 | 95 | 40 | 14 | 1 | 2 | 1 | 337 |
| **Average** | **8.7** | **30.3** | **50.7** | **57.5** | **63** | **24.9** | **7.4** | **2.5** | **1.4** | **1** | **267.9** |
| | | | | | | | | | | | |
| SKN-1gf-1 | 0 | 33 | 35 | 55 | 32 | 23 | 14 | 6 | 0 | 6 | 204 |
| SKN-1gf-2 | 0 | 22 | 39 | 37 | 60 | 16 | 4 | 2 | 1 | 2 | 183 |
| SKN-1gf-3 | 0 | 22 | 44 | 55 | 70 | 42 | 20 | 16 | 23 | 12 | 304 |
| SKN-1gf-4 | 3 | 43 | 58 | 63 | 68 | 18 | 13 | 1 | 0 | 1 | 268 |
| SKN-1gf-5 | 0 | 47 | 54 | 60 | 63 | 40 | 16 | 13 | 9 | 13 | 315 |
| SKN-1gf-6 | 0 | 18 | 41 | 48 | 49 | 55 | 35 | 21 | 13 | 22 | 302 |
| SKN-1gf-7 | 0 | 29 | 45 | 25 | 51 | 16 | 14 | 4 | 0 | 7 | 191 |
| SKN-1gf-8 | 4 | 34 | 47 | 31 | 57 | 43 | 22 | 3 | 3 | 0 | 244 |
| SKN-1gf-9 | 0 | 18 | 34 | 53 | 19 | 38 | 30 | 22 | 8 | 20 | 242 |
| SKN-1gf-10 | 0 | 21 | 40 | 52 | 50 | 27 | 19 | 19 | 6 | 13 | 247 |
| **Average** | **0.7** | **28.7** | **43.7** | **47.9** | **51.9** | **31.8** | **18.7** | **10.7** | **6.3** | **9.6** | **250** |

**1. Animals displaying Bag and Pvl phenotypes or escaped the plate were censored.**

**Table S2. Daily progeny production for wild type and SKN-1gf on the HT115 diet**

| | **Hours post feeding (hpf)** | | | | | | | | | | |
|---|---|---|---|---|---|---|---|---|---|---|---|
| | **60** | **72** | **84** | **96** | **108** | **120** | **132** | **144** | **156** | **168** | **TOTAL** |
| WT-1 | 72 | 121 | 94 | 34 | 11 | 0 | 1 | 0 | 0 | 0 | 333 |
| WT-2 | 60 | 119 | 130 | 55 | 1 | 0 | 0 | 0 | 0 | 0 | 365 |
| WT-3 | 86 | 107 | 123 | 72 | 4 | 2 | 0 | 0 | 0 | 0 | 394 |
| WT-4 | 75 | 114 | 119 | 48 | 4 | 0 | 0 | 0 | 0 | 0 | 360 |
| WT-5 | 77 | 121 | Censored[1] | | | | | | | | 258 |
| WT-6 | 80 | 105 | 98 | 47 | 1 | 0 | 0 | 0 | 0 | 0 | 331 |
| WT-7 | 73 | 115 | 79 | 22 | 3 | 0 | 0 | 0 | 0 | 0 | 292 |
| WT-8 | 59 | Censored[1] | | | | | | | | | 115 |
| WT-9 | 90 | 127 | 81 | 6 | 0 | 0 | 0 | 0 | 0 | 0 | 304 |
| WT-10 | 77 | 112 | 67 | 14 | 11 | 2 | 0 | 0 | 0 | 0 | 283 |
| **Average** | **74.9** | **109.7** | **85** | **29.8** | **3.6** | **0.4** | **0.1** | **0** | **0** | **0** | **332.8** |
| | | | | | | | | | | | |
| SKN-1gf-1 | 47 | 82 | 72 | 36 | 1 | 5 | 1 | 0 | 0 | 0 | 244 |
| SKN-1gf-2 | 64 | 105 | 108 | 41 | 4 | 0 | 0 | 0 | 0 | 0 | 322 |
| SKN-1gf-3 | 47 | 112 | 116 | 58 | 17 | 0 | 0 | 0 | 0 | 0 | 350 |
| SKN-1gf-4 | 58 | 102 | 97 | 33 | 0 | 0 | 0 | 0 | 0 | 0 | 290 |
| SKN-1gf-5 | 63 | 85 | 87 | 17 | 3 | 2 | 0 | 0 | 0 | 0 | 257 |
| SKN-1gf-6 | 49 | 66 | Censored[1] | | | | | | | | 188 |
| SKN-1gf-7 | 50 | 100 | 105 | 54 | 7 | 0 | 0 | 0 | 0 | 0 | 316 |
| SKN-1gf-8 | 64 | 96 | 90 | 45 | 7 | 0 | 0 | 0 | 0 | 0 | 302 |
| SKN-1gf-9 | 59 | 105 | 104 | 52 | 7 | 0 | 0 | 0 | 0 | 0 | 327 |
| SKN-1gf-10 | 51 | 124 | 108 | 39 | 0 | 0 | 0 | 0 | 0 | 0 | 322 |
| **Average** | **55.2** | **97.7** | **94.6** | **38.8** | **4.7** | **0.7** | **0.1** | **0** | **0** | **0** | **291.8** |

**1. Animals displaying Bag and Pvl phenotypes or escaped the plate were censored.**

**Table S3**. **OP50 RNAi knockdown efficiencies**

| Gene | Description[1] | Expression | Significance[3] |
|---|---|---|---|
| *skn-1* | bZip transcription factor orthologous to the mammalian Nrf (Nuclear factor-erythroid-related factor) | 0.609 | * |
| *gst-4* | SKN-1 target used as second assessment of *skn-1* RNAi efficacy | 0.100 | *** |
| *fat-6* | delta-9 fatty acid desaturase | 0.068 | *** |
| *fat-7* | delta-9 fatty acid desaturase | 0.084 | *** |
| *vit-2* | vitellogenin homolog YP170 | 0.344 | ** |

1. Gene descriptions provided by WormBase version: WS249

2. mRNA expression levels in SKN-1gf animals treated with indicated RNAi relative to SKN-1gf animals treated with vector control RNAi; normalized to *snb-1* expression as a control, which was invariant across samples. Green and red color indicates increased and decreased expression, respectively.

3. *, *P*-value<0.05; **, *P*-value<0.01; ****, *P*-value<0.0001; n.s., difference between samples in non significant = *P*-value>0.05

**Table S4**. **mRNA expression levels of oleic acid and eicosanoid biosynthesis pathway genes**

| Target | Description[1] | Fold-change[2] | Significance[3] |
|---|---|---|---|
| *gst-4* | Control for SKN-1 activation | 36.76 | **** |
| *fat-1* | omega-3 fatty acyl desaturase | -1.31 | * |
| *fat-4* | delta-5 fatty acid desaturase | -1.35 | n.s. |
| *fat-6* | delta-9 fatty acid desaturase | -1.21 | n.s. |
| *fat-7* | delta-9 fatty acid desaturase | -1.91 | *P*=0.05 |

1. Gene descriptions provided by WormBase version: WS249

2. Fold-change in expression in SKN-1gf mutant animals relative to wild-type animals normalized to *snb-1* expression as a control, which was invariant across samples. Green and red color indicates increased and decreased expression, respectively.

3. *, *P*-value<0.05; **, *P*-value<0.01; ****, *P*-value<0.0001; n.s., difference between samples in non significant = *P*-value>0.05

**Table S5. Variation of Asdf phenotype among natural isolates of *C. elegans*.**

| Strain[1] | Location isolated[2] | Asdf[3] |
|---|---|---|
| NL7000 | Bergerac, France | +++ |
| ED3040 | Johannesburg, South Africa | +++ |
| ED3021 | Edinburgh, Scotland | ++ |
| ED3049 | Ceres, South Africa | + |
| RW7000 | Bergerac, France | - |
| TR403 | Wisconsin, USA | - |
| CB4869 | Vancouver, Canada | - |
| CB4856 | Hawaii, USA | - |

1. Strain designation as reported to the *Caenorhabditis* Genetics Center (CGC)
2. Geographic location where strain was isolated (Wormbase)
3. Penetrance of Asdf phenotype. -, not observed; +, 25-50% of population display Asdf, ++, 50-75% of population display Asdf; +++, 75-100% of population display Asdf.

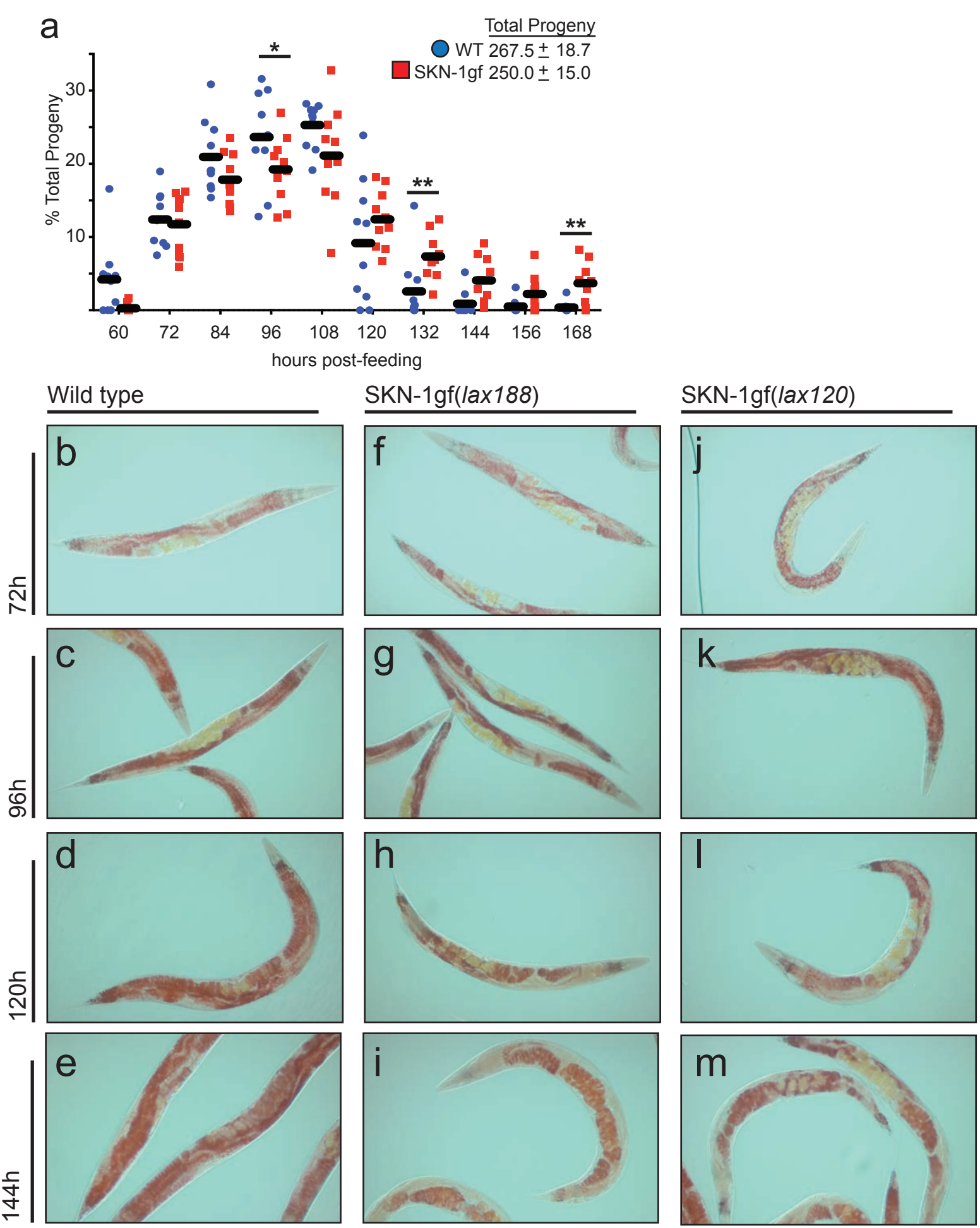


Lynn et al.
Figure S1

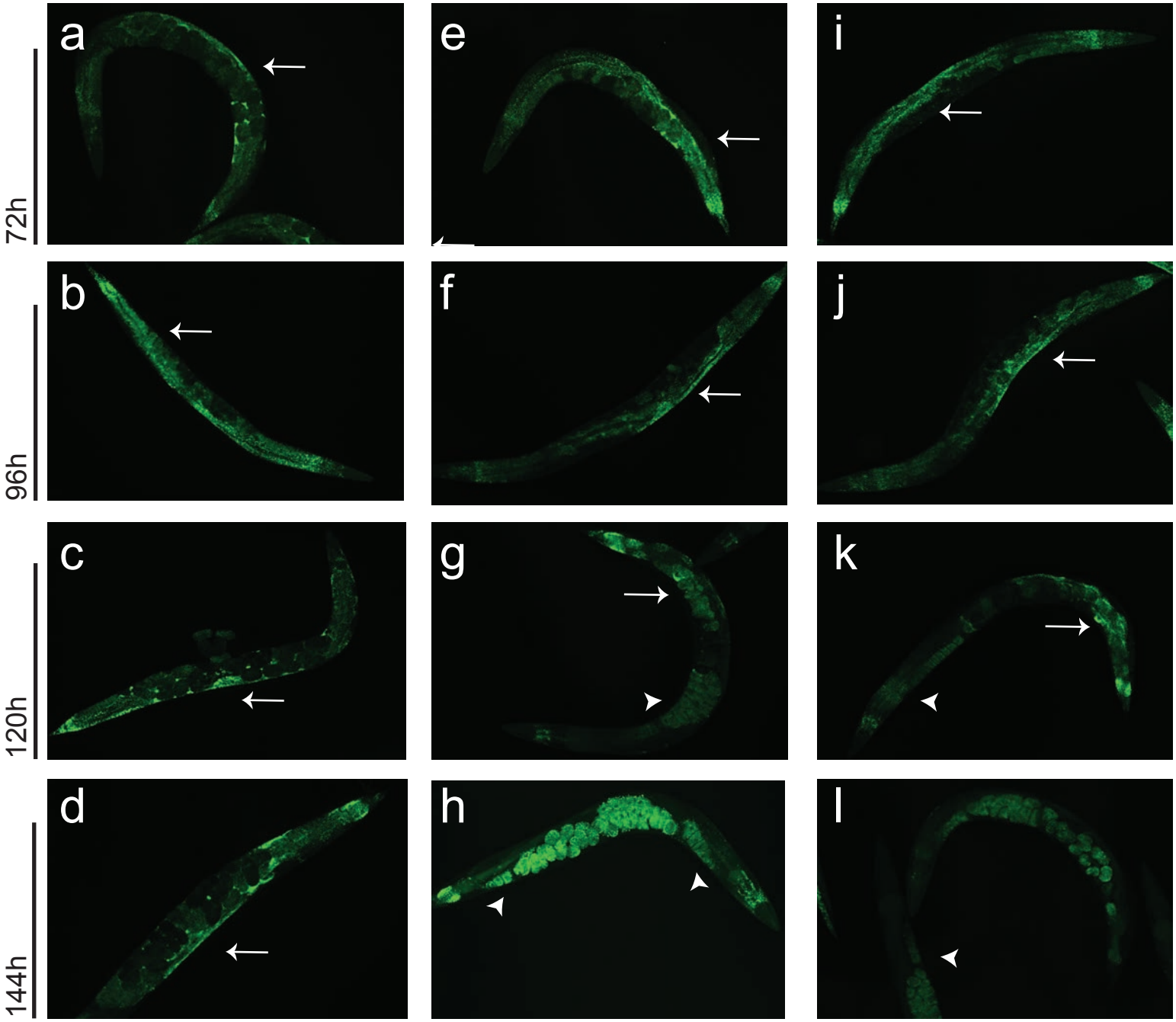


Lynn et al.
Figure S2

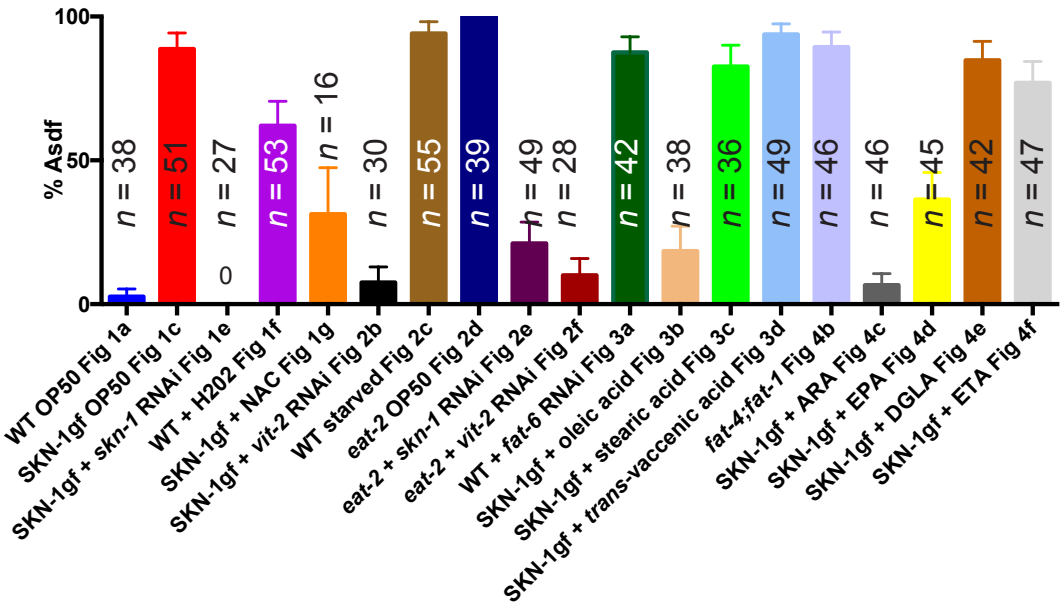


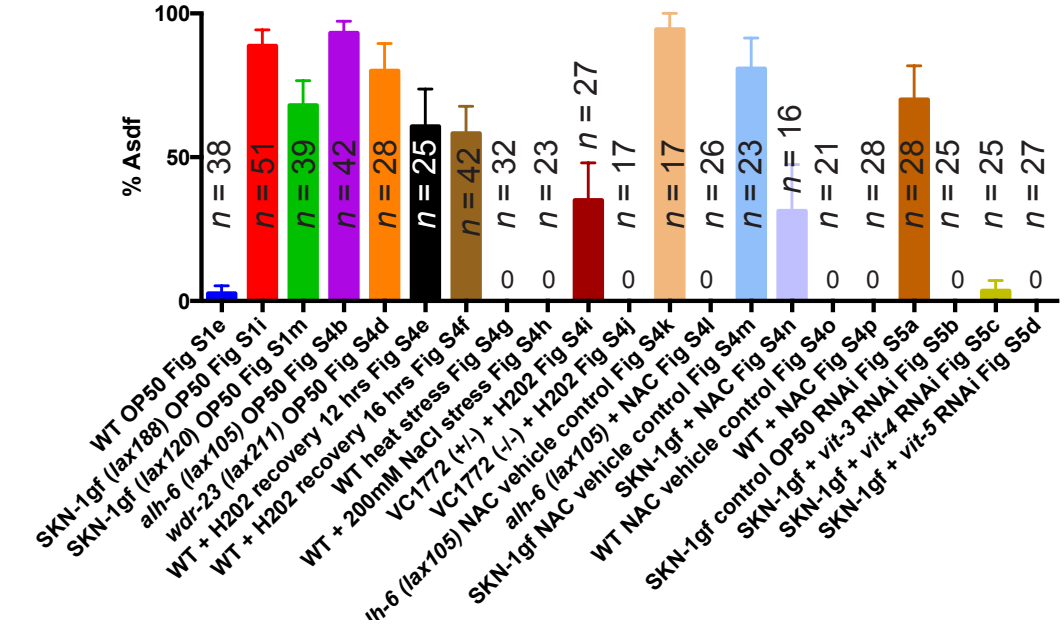


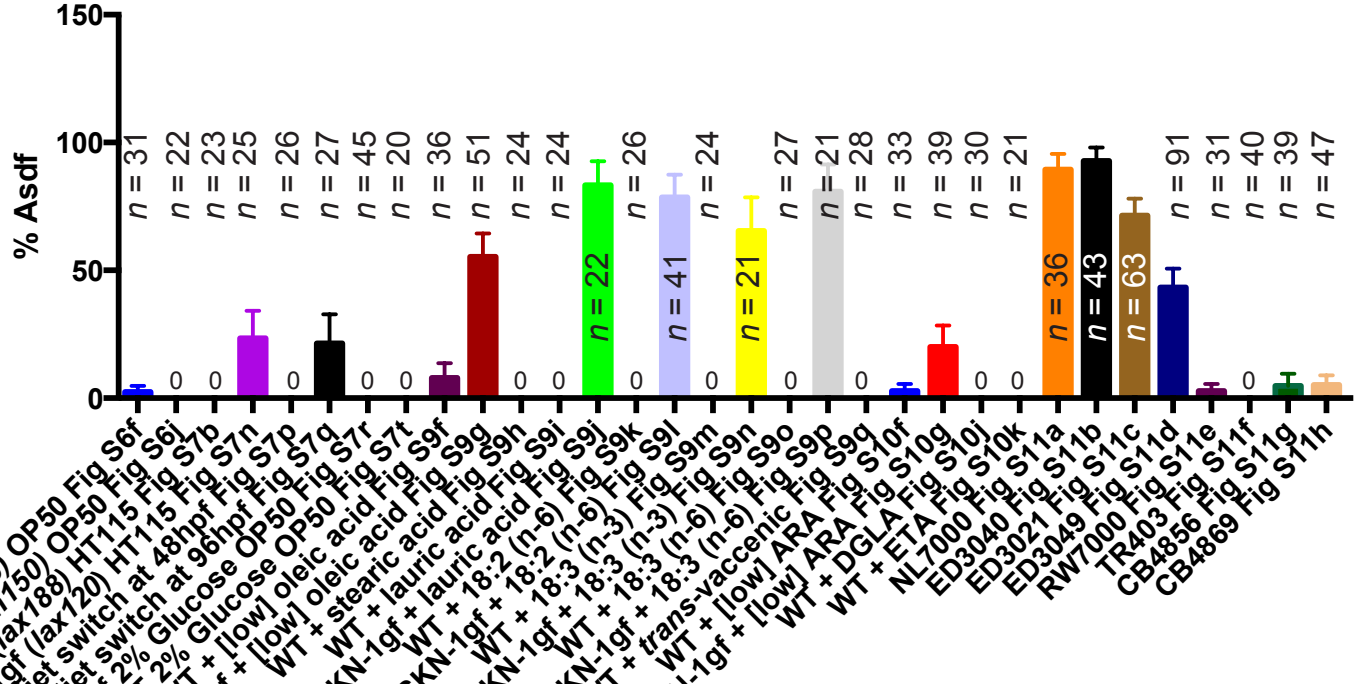


Lynn et al.
Figure S3

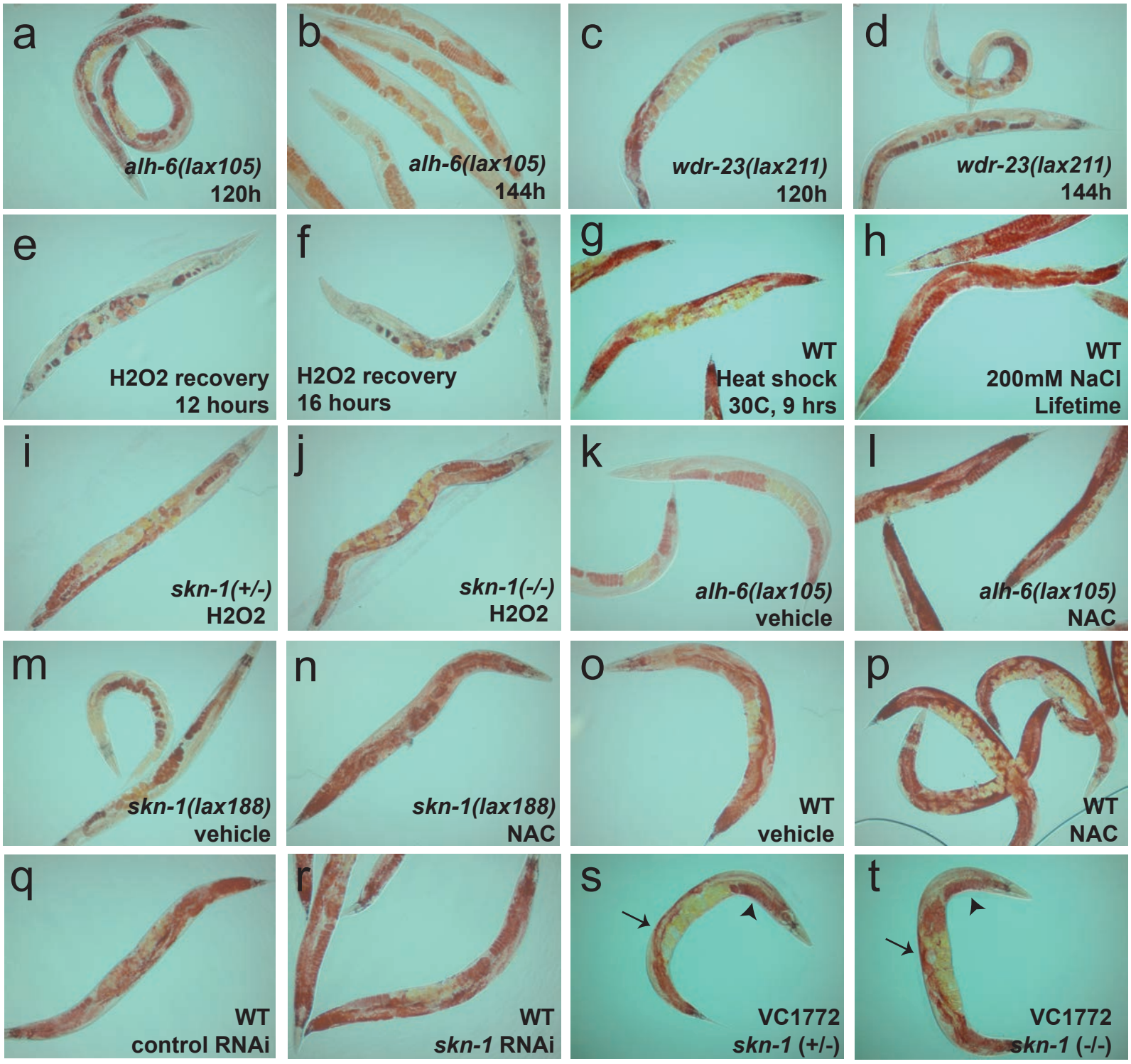


Lynn et al.
Figure S4

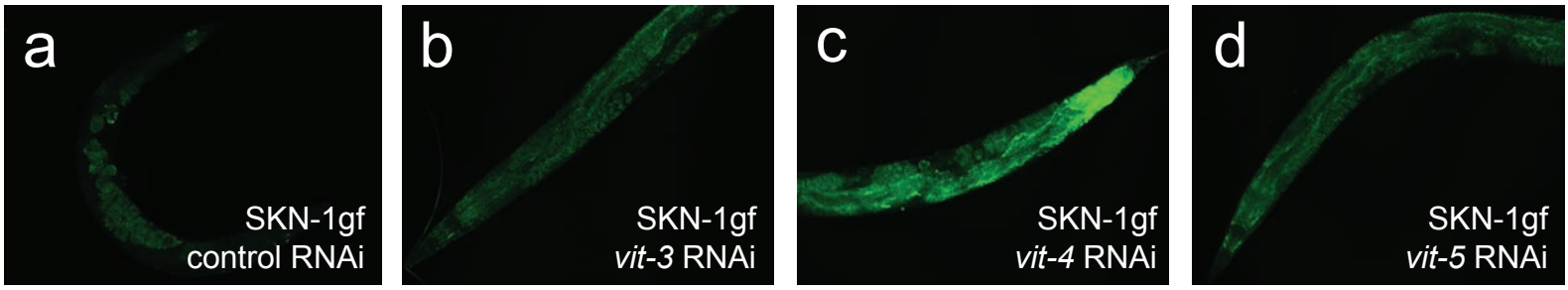


Lynn et al.
Figure S5

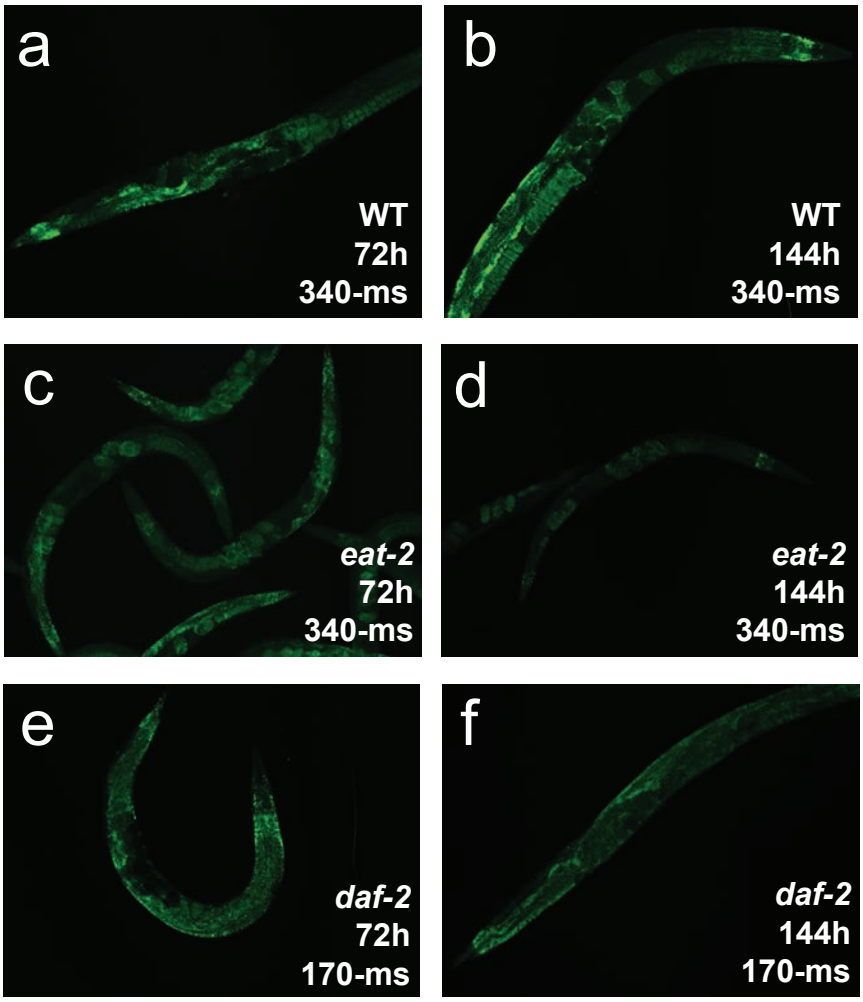


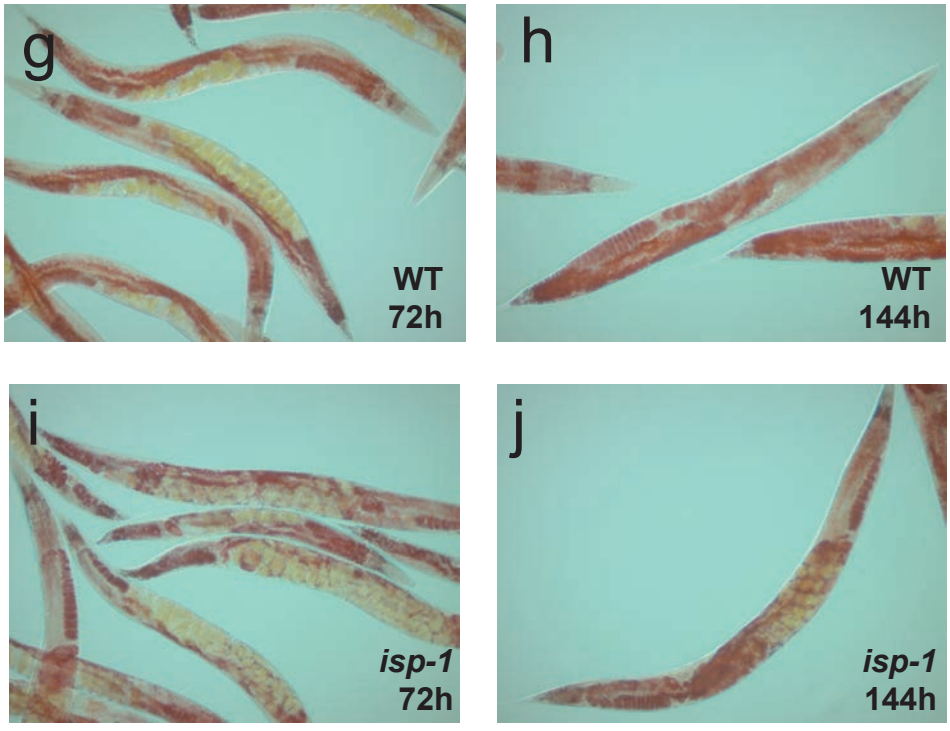


Lynn et al.
Figure S6

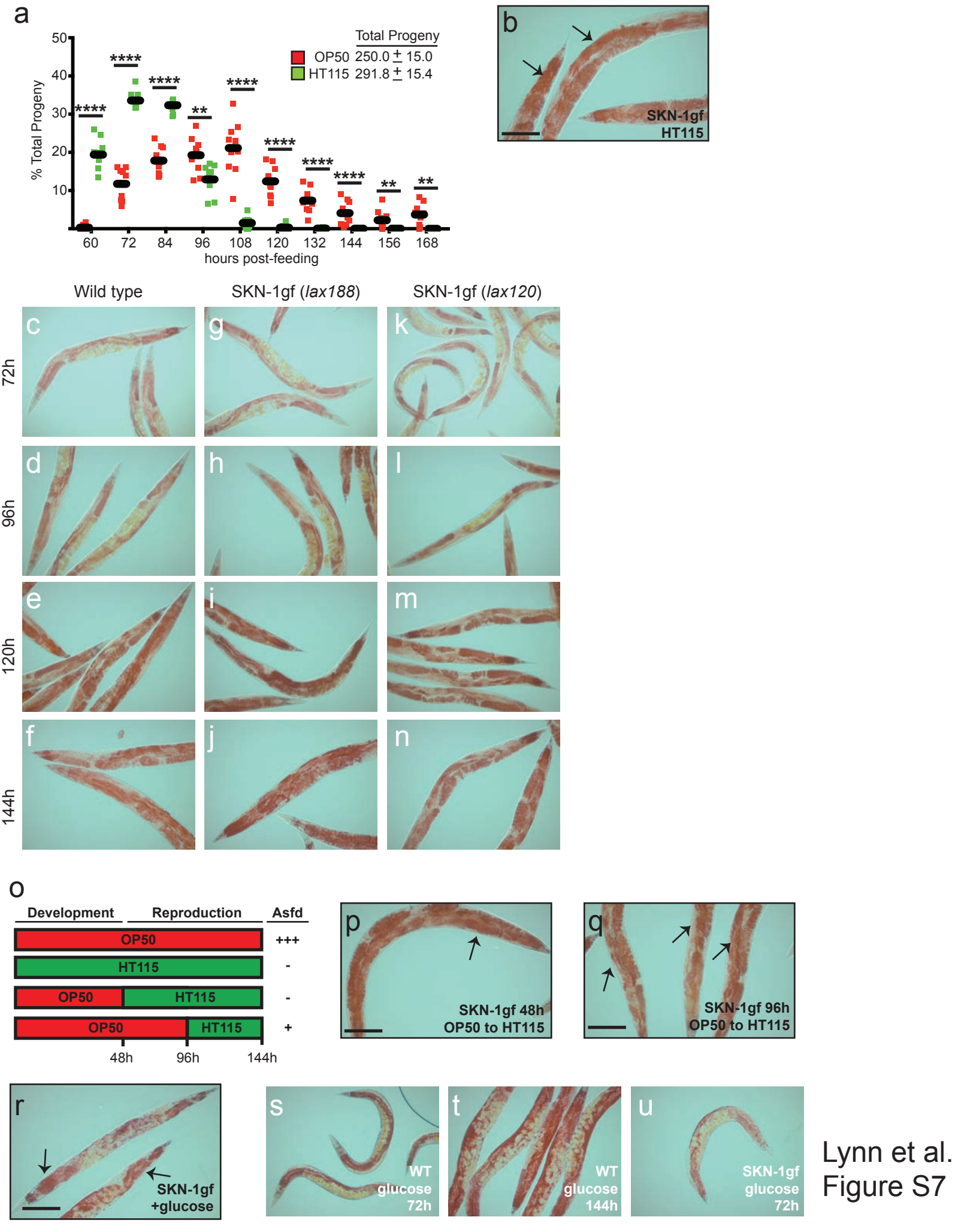


Lynn et al.
Figure S7

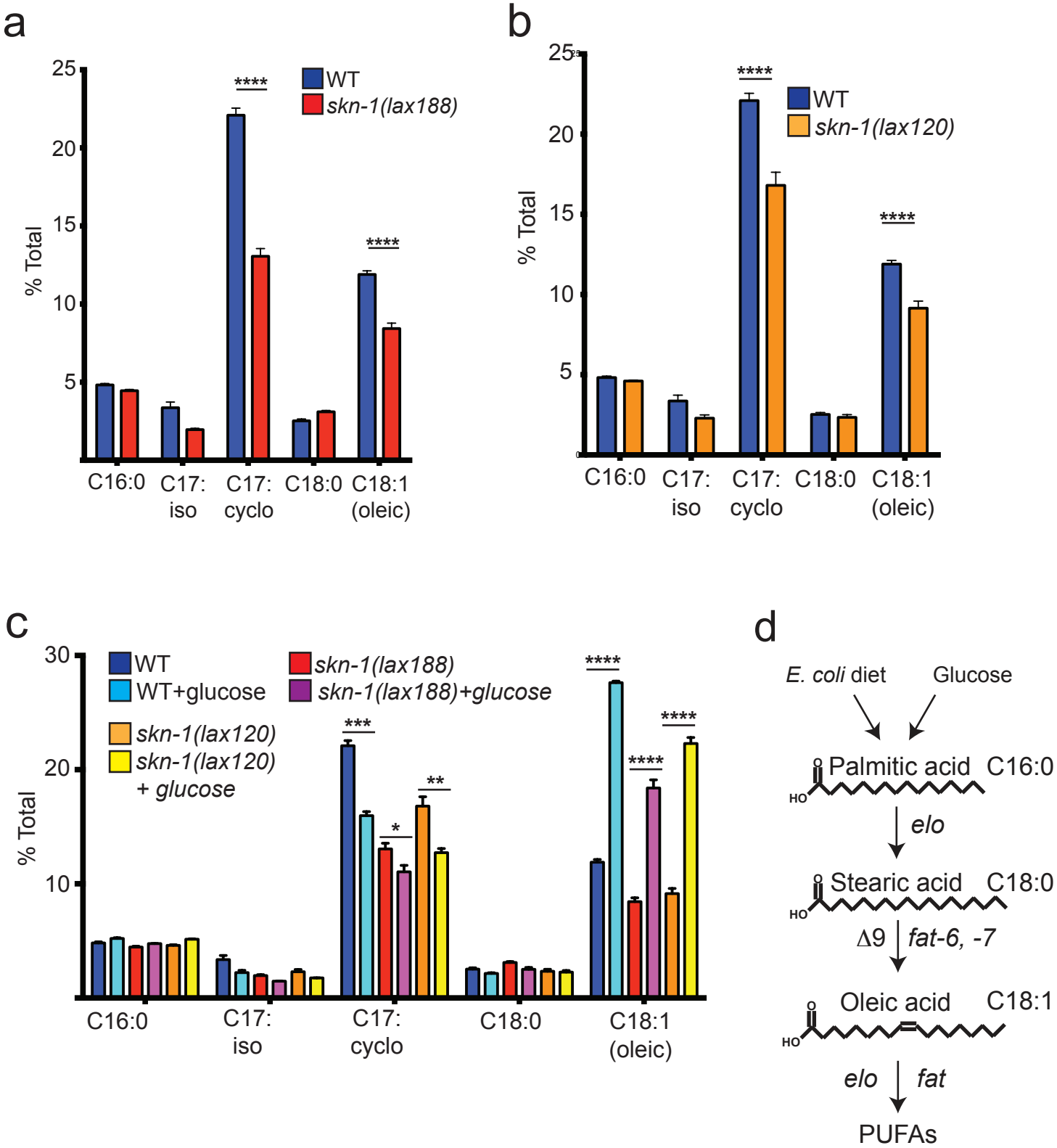


Lynn et al.
Figure S8

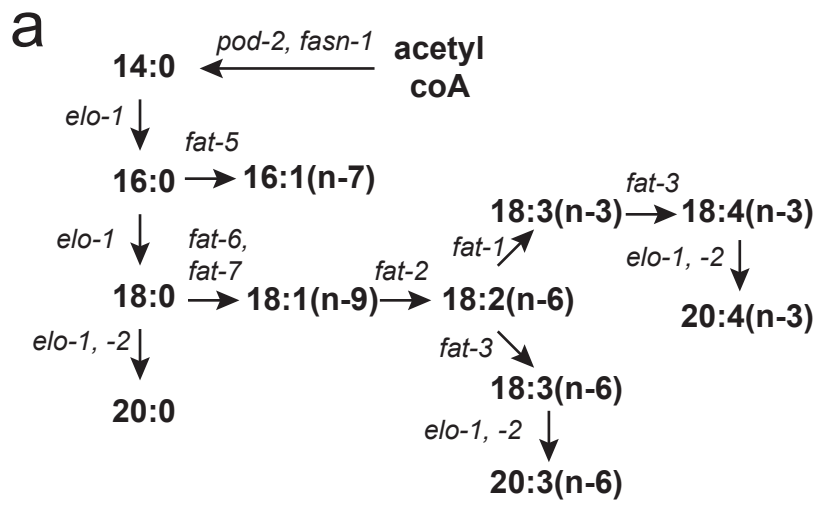


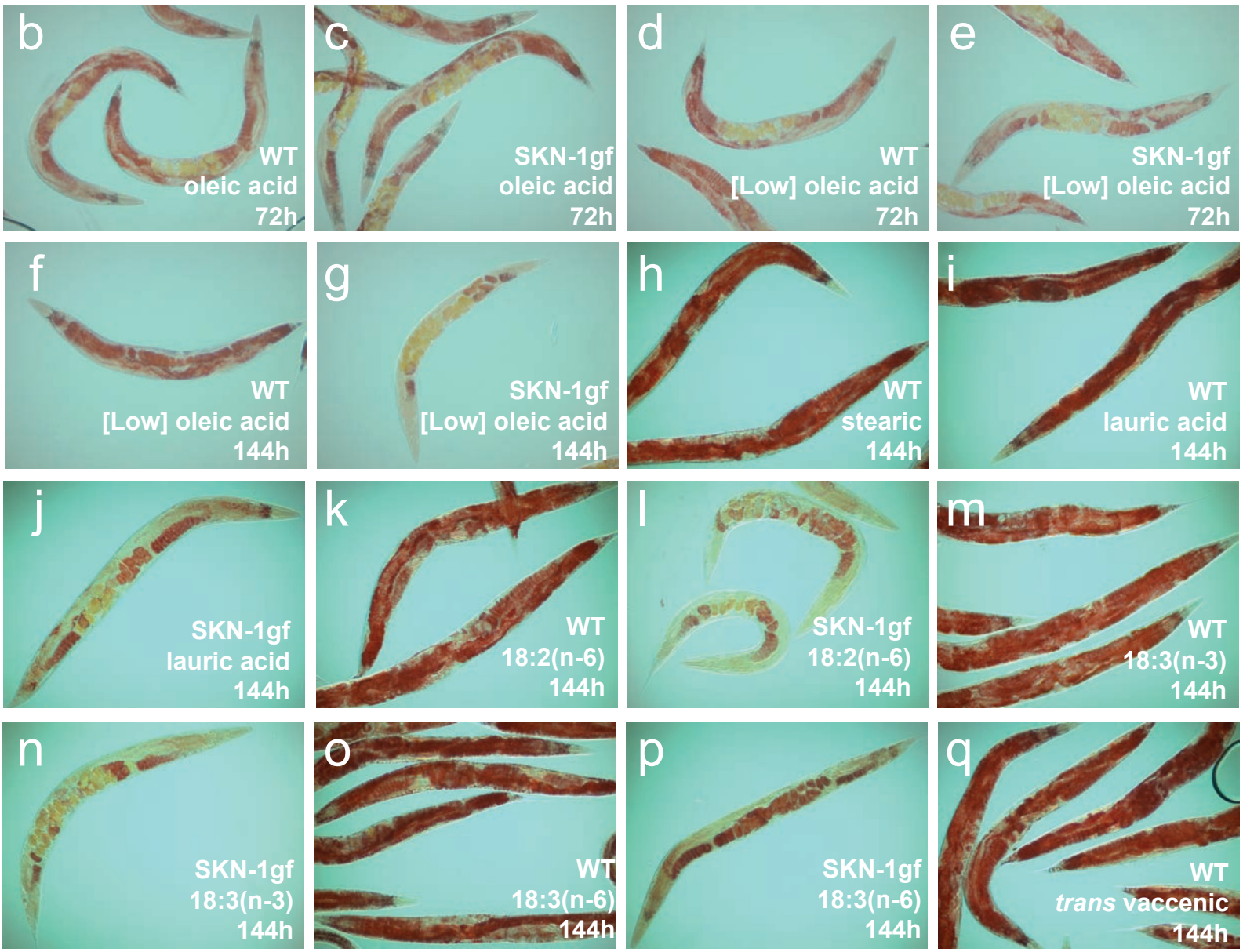


Lynn et al.
Figure S9

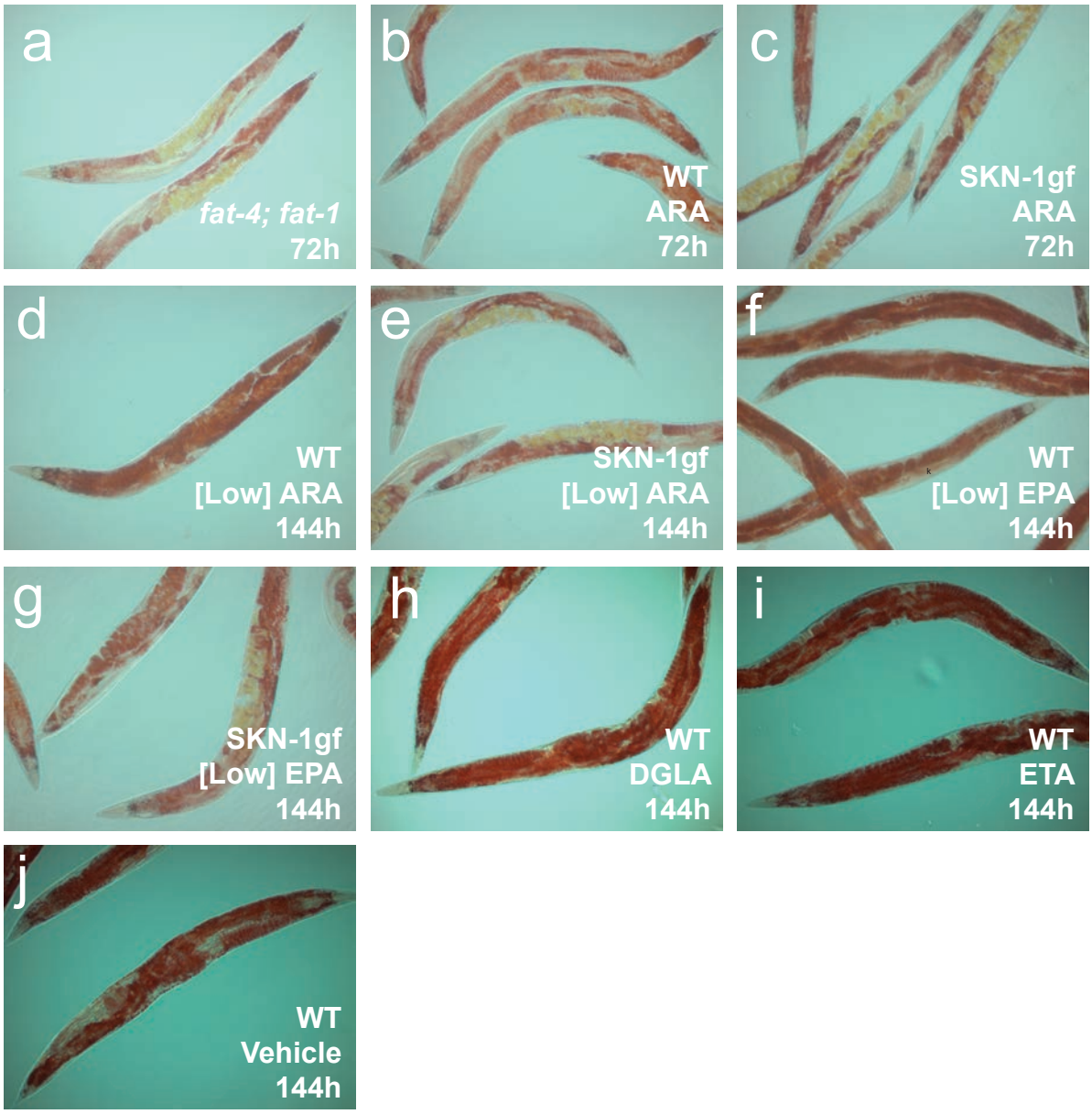


Lynn et al.
Figure S10

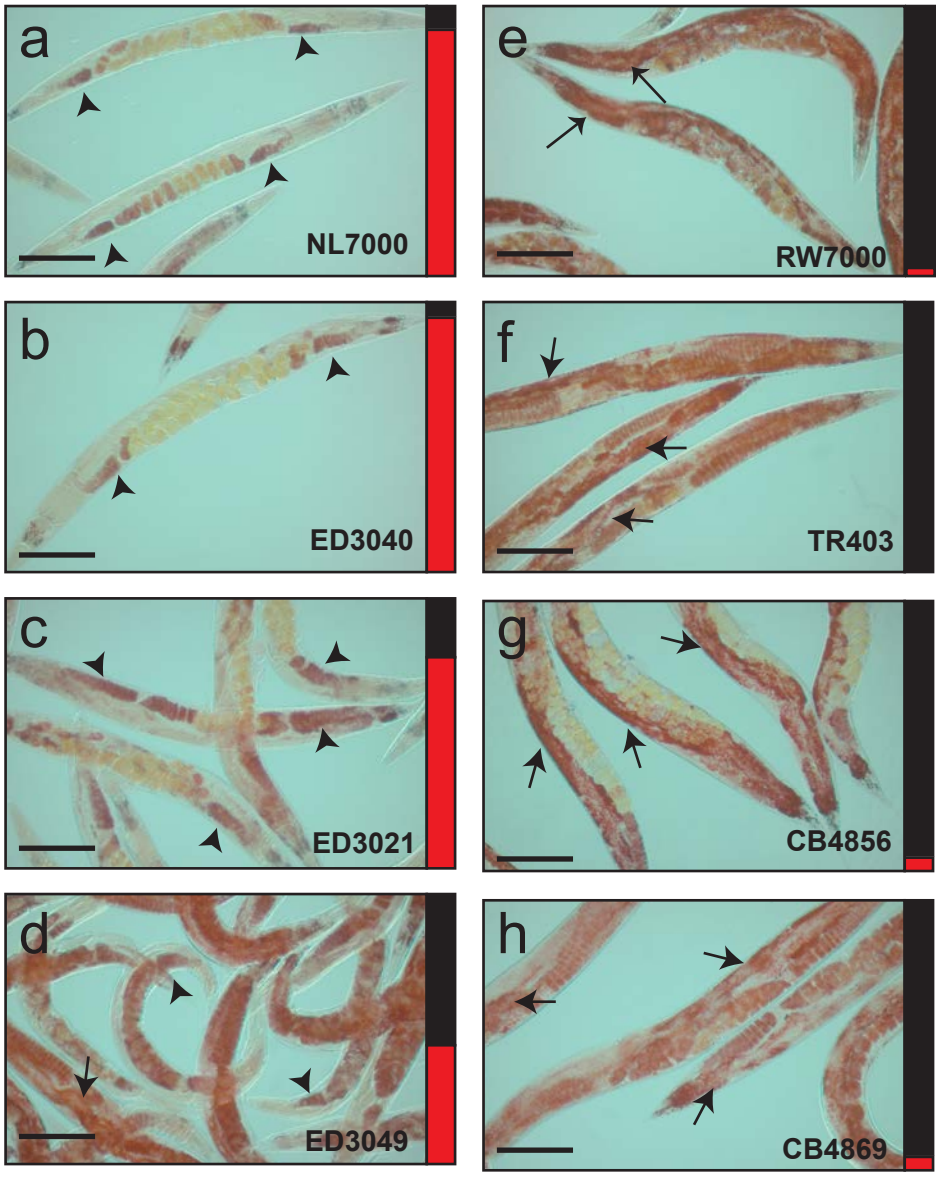


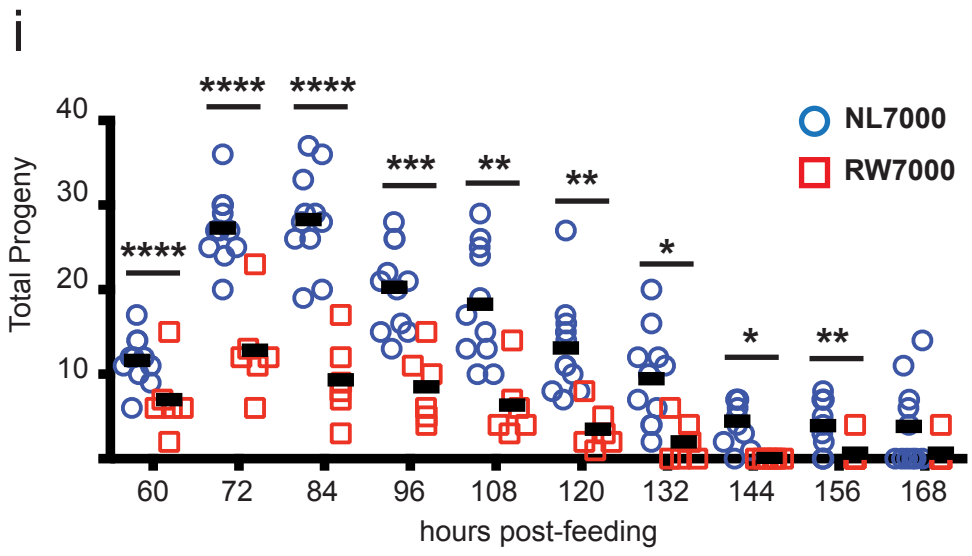


Lynn et al.
Figure S11

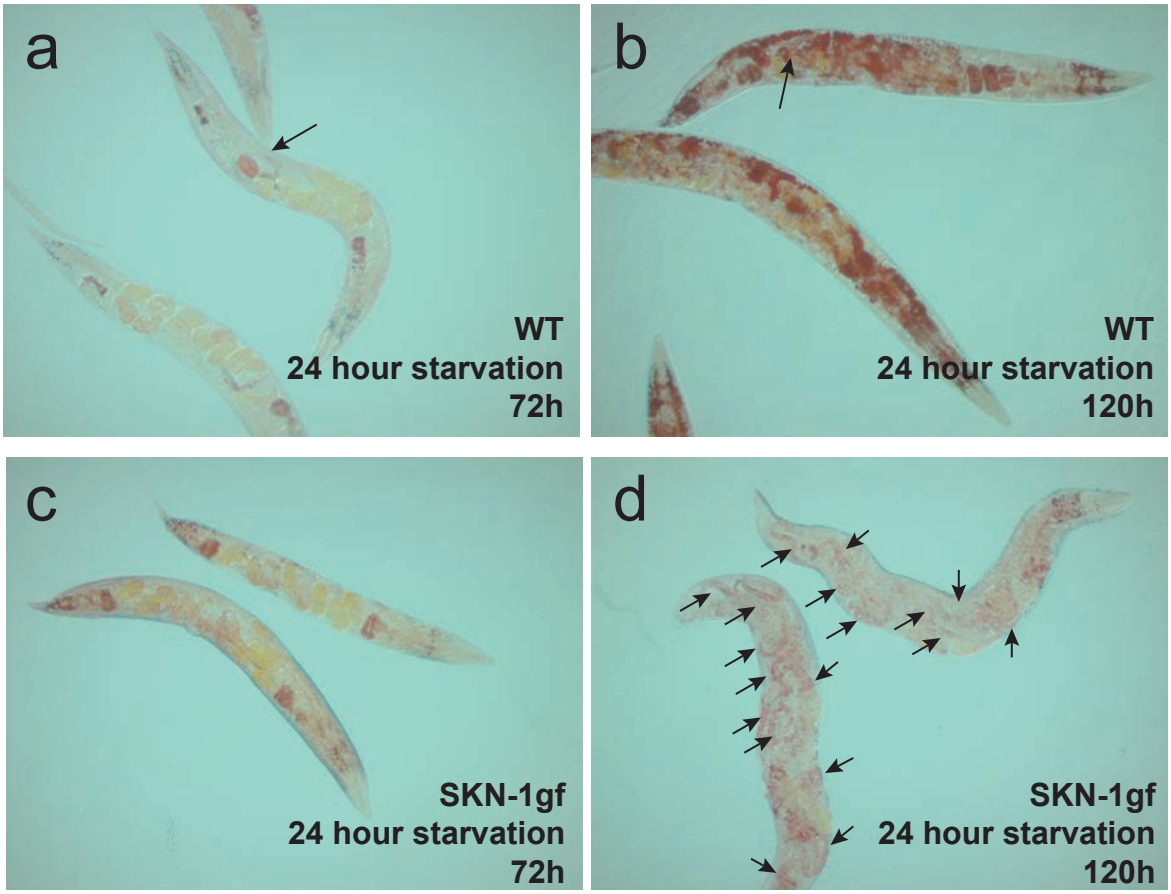


Lynn et al.
Figure S12

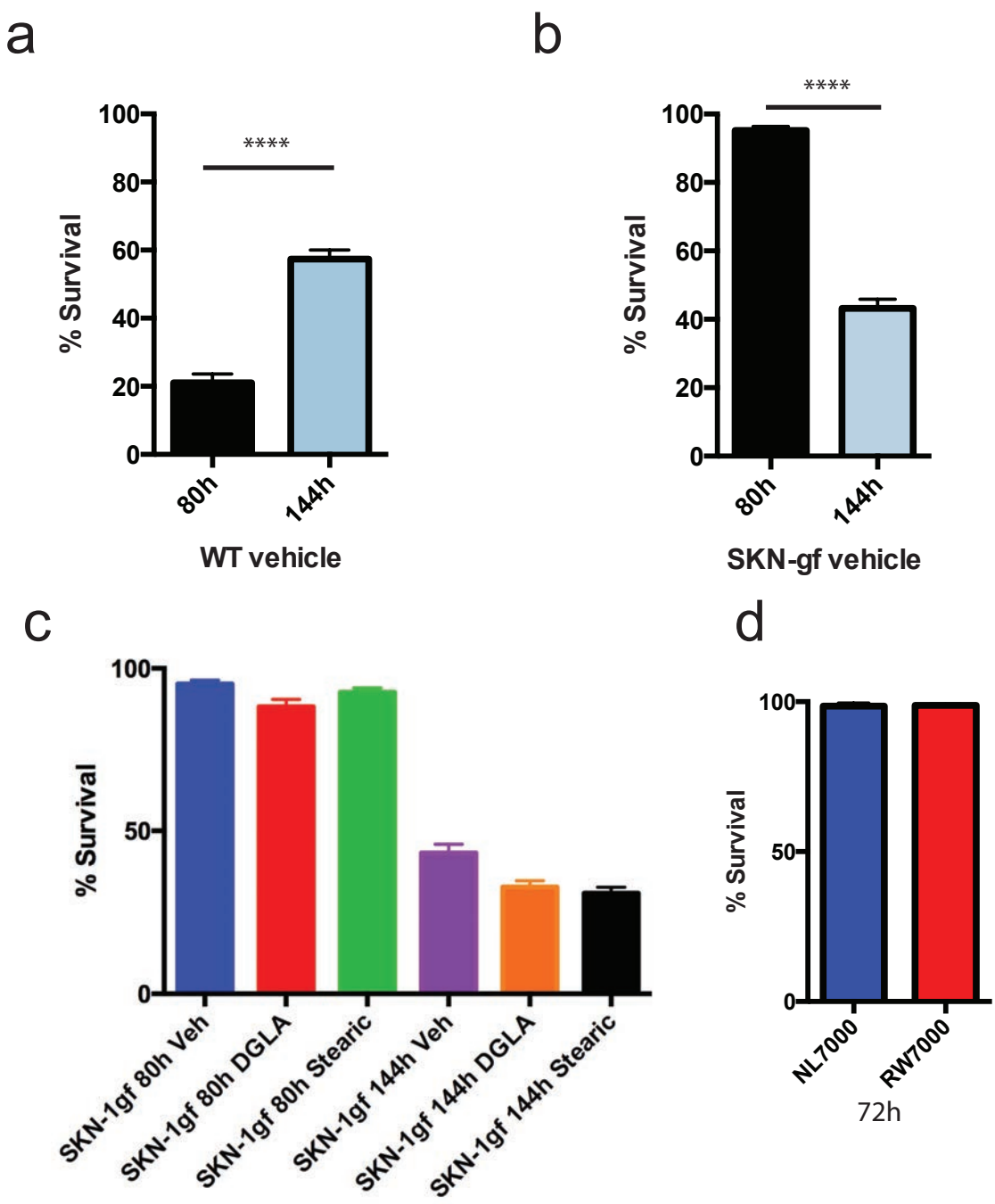


Lynn et al.
Figure S13